

# C<sub>4</sub> and crassulacean acid metabolism within a single leaf: deciphering key components behind a rare photosynthetic adaptation

Renata C. Ferrari<sup>1</sup> , Priscila P. Bittencourt<sup>1</sup>, Maria A. Rodrigues<sup>1</sup>, Jose J. Moreno-Villena<sup>2</sup>, Frederico R. R. Alves<sup>1</sup> , Vinícius D. Gastaldi<sup>3</sup> , Susanna F. Boxall<sup>4</sup> , Louisa V. Dever<sup>4</sup> , Diego Demarco<sup>1</sup> , Sônia C.S. Andrade<sup>5</sup> , Erika J. Edwards<sup>2</sup>, James Hartwell<sup>4</sup>  and Luciano Freschi<sup>1</sup> 

<sup>1</sup>Departamento de Botânica, Instituto de Biociências, Universidade de São Paulo, São Paulo 05508-090, Brasil; <sup>2</sup>Department of Ecology and Evolutionary Biology, Yale University, PO Box 208105, New Haven, CT 06520, USA; <sup>3</sup>Departamento e Instituto de Psiquiatria, Hospital das Clínicas (HCFMUSP), Faculdade de Medicina, Universidade de São Paulo, São Paulo 05403-903, Brasil; <sup>4</sup>Department of Functional and Comparative Genomics, Institute of Integrative Biology, University of Liverpool, Liverpool, L69 7ZB, UK; <sup>5</sup>Departamento de Genética e Biologia Evolutiva, Instituto de Biociências, Universidade de São Paulo, São Paulo 05508-090, Brasil

## Summary

Authors for correspondence:

Luciano Freschi

Tel: +55 11 3091 8068

Email: freschi@usp.br

James Hartwell

Tel: +44 (0)151 795 4561

Email: james.hartwell@liverpool.ac.uk

Received: 17 July 2019

Accepted: 7 October 2019

New Phytologist (2020) 225: 1699–1714

doi: 10.1111/nph.16265

**Key words:** C<sub>4</sub>, crassulacean acid metabolism, drought stress, facultative CAM, *Portulaca oleracea*, RNA-seq, transcriptome.

- Although biochemically related, C<sub>4</sub> and crassulacean acid metabolism (CAM) systems are expected to be incompatible. However, *Portulaca* species, including *P. oleracea*, operate C<sub>4</sub> and CAM within a single leaf, and the mechanisms behind this unique photosynthetic arrangement remain largely unknown.
- Here, we employed RNA-seq to identify candidate genes involved exclusively or shared by C<sub>4</sub> or CAM, and provided an in-depth characterization of their transcript abundance patterns during the drought-induced photosynthetic transitions in *P. oleracea*. Data revealed fewer candidate CAM-specific genes than those recruited to function in C<sub>4</sub>. The putative CAM-specific genes were predominantly involved in night-time primary carboxylation reactions and malate movement across the tonoplast. Analysis of gene transcript-abundance regulation and photosynthetic physiology indicated that C<sub>4</sub> and CAM coexist within a single *P. oleracea* leaf under mild drought conditions.
- Developmental and environmental cues were shown to regulate CAM expression in stems, whereas the shift from C<sub>4</sub> to C<sub>4</sub>-CAM hybrid photosynthesis in leaves was strictly under environmental control. Moreover, efficient starch turnover was identified as part of the metabolic adjustments required for CAM operation in both organs.
- These findings provide insights into C<sub>4</sub>/CAM connectivity and compatibility, contributing to a deeper understanding of alternative ways to engineer CAM into C<sub>4</sub> crop species.

## Introduction

C<sub>4</sub> and crassulacean acid metabolism (CAM) are two major carbon (C)-concentrating mechanisms (CCMs) in higher plants (Hatch, 1987; Griffiths, 1989; Keeley & Rundel, 2003). C<sub>4</sub> occurs in *c.* 19 families, mostly distributed in hot and high-light environments (Sage, 2017). It relies on the spatial separation between primary CO<sub>2</sub> assimilation by phosphoenolpyruvate carboxylase (PPC) in mesophyll cells (MCs) and secondary refixation by ribulose 1,5-bisphosphate carboxylase/oxygenase (Rubisco) in bundle sheath cells (BSCs) (Laetsch, 1968; Kanai & Edwards, 1999), being usually associated with Kranz anatomy (Voznesenskaya *et al.*, 2001, 2002). Besides increasing photosynthetic rates and suppressing photorespiration, C<sub>4</sub> can increase water-use efficiency (WUE) relative to C<sub>3</sub> as lower stomatal conductance is required for a given assimilation rate (Taylor *et al.*, 2014).

Crassulacean acid metabolism is found in at least 35 families mainly distributed in arid environments (Winter, 2019), and is also commonly, but not exclusively, associated with higher leaf succulence (Nelson *et al.*, 2005; Silvera *et al.*, 2010; Edwards 2019). In contrast to C<sub>4</sub>, CAM occurs in each individual MC and relies on temporal coordination of primary and secondary CO<sub>2</sub> fixation by the circadian clock (Hartwell, 2006). In strong CAM plants, stomatal opening and, consequently, atmospheric CO<sub>2</sub> uptake and C<sub>4</sub> acid formation are rescheduled to the dark period, when transpiration rates are lower, whereas stomata close for much of the light period, preventing water loss and increasing WUE (Osmond, 1978; Borland *et al.*, 2009). The dark CO<sub>2</sub> fixation by PPC and the daytime refixation of CO<sub>2</sub> by Rubisco characterize CAM phases I and III, respectively, with additional transitional phases at dawn and dusk (phases II and IV, respectively) where stomata can also be open, allowing direct fixation of

atmospheric CO<sub>2</sub> by Rubisco (Winter & Smith, 1996). Crassulacean acid metabolism also differs from C<sub>4</sub> in its variability of expression, as many facultative plants operate CAM under stress (e.g. drought), but perform C<sub>3</sub> photosynthesis whenever conditions allow (Winter & Holtum, 2014). Crassulacean acid metabolism is weakly expressed in many facultative species, as nocturnal CO<sub>2</sub> fixation under stress conditions contribute < 5% compared with daytime CO<sub>2</sub> fixation via C<sub>3</sub> under optimal growth conditions (Winter, 2019).

A set of biochemical reactions are shared by C<sub>4</sub> and CAM, including many involved in carboxylation and decarboxylation steps (Bräutigam *et al.*, 2017), as both CCMs depend on the formation of four-C organic acids to store, transport and release CO<sub>2</sub> in the vicinity of Rubisco (Edwards & Ogburn, 2012). Post-translational regulatory steps are also shared in C<sub>4</sub> and CAM species, including the phosphorylation-dependent control of PPC and pyruvate, orthophosphate dikinase (PPDK) activities by PPC kinase (PPCK) and PPDK regulatory protein (PPDKRP), respectively (Nimmo *et al.*, 2001; Chastain & Chollet, 2003; Dever *et al.*, 2015). However, while C<sub>4</sub> requires specific metabolites, transporters and decarboxylases (Kanai & Edwards, 1999; Schluter *et al.*, 2016), CAM relies on strict temporal coordination of primary and secondary CO<sub>2</sub> fixation and appropriate transporters for acid import and export from the vacuole (Winter & Smith, 1996; Hartwell *et al.*, 2016). Differently from C<sub>4</sub> species, a dedicated pool of carbohydrates (starch or soluble sugars, depending on the species) is converted into phosphoenolpyruvate (PEP) via glycolysis each night to sustain PPC activity in CAM (Black *et al.*, 1996; Weise *et al.*, 2011). Moreover, a change from the hydrolytic to the phosphorolytic starch breakdown pathway is usually observed during CAM induction in facultative species (Borland *et al.*, 2016).

C<sub>4</sub> and CAM are believed to be incompatible to occur in the same cell, as each CCM requires potentially conflicting regulatory processes, metabolic fluxes and structural arrangements (Sage, 2002). However, the occurrence of both CCMs within a single leaf is rare, but possible, as observed in *Portulaca* spp. (Sage, 2002; Winter, 2019). Species from all main *Portulaca* lineages have been reported to induce CAM in response to drought (Koch & Kennedy, 1980, 1982; Ku *et al.*, 1981; Guralnick & Jackson, 2001; Holtum *et al.*, 2017; Winter & Holtum, 2017; Winter *et al.*, 2019). Among them, *P. oleracea* L. displays rapid growth, high seed production (up to 200 000 seeds per plant), a cosmopolitan distribution, and is economically important as food and medicine (Zimmerman, 1976; Miyanishi & Cavers, 1980; Gonnella *et al.*, 2010). *Portulaca oleracea*, therefore, represents an attractive model for the study of the C<sub>4</sub>-CAM compatibility in leaves (Hartwell *et al.*, 2016; Ferrari & Freschi, 2019). Moreover, stems are also photosynthetic in this species, and can accumulate acids overnight under drought (Koch & Kennedy, 1980), but are devoid of C<sub>4</sub> anatomical attributes (Voznesenskaya *et al.*, 2010).

Both C<sub>4</sub> and CAM are relevant targets for forward genetic engineering into C<sub>3</sub> crop species as a result of their natural ability to outperform C<sub>3</sub> plants in hotter and drier environments. Attempts are underway to engineer the C<sub>4</sub> pathway into rice, such as the C<sub>4</sub> Rice Initiative (Kajala *et al.*, 2011; Covshoff &

Hibberd, 2012), and to transfer CAM into C<sub>3</sub> food and bioenergy crops (Borland *et al.*, 2009; Yang *et al.*, 2015; Hartwell *et al.*, 2016). From this perspective, *P. oleracea* provides a potentially unique genetic blueprint of how C<sub>4</sub> and CAM can occur within a single leaf. As such, unraveling the components behind this rare photosynthetic adaptation may provide valuable insights that can guide and inform the challenge of bioengineering facultative CAM into C<sub>4</sub> crops, combining high productivity under optimum growth conditions and increased survival during intermittent drought events (Ferrari & Freschi, 2019).

In this study, we report the gene transcript abundance and metabolic changes associated with the modulation of C<sub>4</sub> and CAM expression in *P. oleracea* plants challenged by alterations in water availability. We focused on the identification of components that were either exclusive to or shared by C<sub>4</sub> and/or CAM pathways. Our results revealed that inducible CAM in *P. oleracea* requires the upregulation of relatively few CCM genes, and that the induction of these genes can be controlled either by the environment (drought) or by developmental cues, depending on the organ (leaves or stems). Simultaneous C<sub>4</sub> and CAM functioning were observed soon after drought exposure, indicating that both CCMs can coexist within a single leaf. Novel insights are also provided into the additional metabolic adjustments (e.g. sugar metabolism rewiring) and regulatory mechanisms (e.g. transcriptional regulation of key genes) involved in this remarkable photosynthetic adaptation.

## Materials and Methods

### Plant material, growth conditions and sampling

Plants were grown in 25 ml square pots containing commercial substrate and vermiculite at a photosynthetic flux density (PFD) at plant height of 250–300 μmol m<sup>-2</sup> s<sup>-1</sup>, a 12h photoperiod, a 27 ± 1°C : 22 ± 1°C, day : night temperature, and 60 ± 10% : 80 ± 10%, day : night air humidity. After 20–30 d of initial growth, plants were separated into three experimental groups, each one submitted to a different watering regime as follows: plants watered daily (well watered); plants subjected to water withholding until soil volumetric water content (SVWC) reached 10–20% and subsequently maintained at this percentage until sampling (drought-stressed); and plants irrigated to field capacity after 22 and 34 d of drought (rewatered). SVWC was continuously monitored (every 30 min) using Decagon soil moisture meter EC-5 coupled to the Em5b datalogger (Decagon Devices, Pullman, WA, USA). Leaf and stem osmotic potential (Ψ<sub>s</sub>) were monitored at dawn, as described in Supporting Information Methods S1.

Sampling of leaves and stems took place after 0, 10, 22 and 34 d of drought treatment (D0, D1, D2 and D3, respectively), and also 4 d after rewatering events that were initiated at D2 and D3 (R1 and R2, respectively). Samples were harvested 1 h after the onset of illumination (dawn samples) and 1 h before the end of the light period (dusk samples). At D3, leaf and stem samples were also harvested every 4 h over a light : dark cycle starting 2 h after the onset of the light period (08:00, 12:00, 16:00, 20:00,

24:00, 04:00, 08:00 h). Three to four biological replicates, each composing at least three individual plants per replicate, were harvested at each sampling time. All fully expanded and nonsenescent leaves (leaf samples) and whole stems (stem samples) were frozen in liquid N<sub>2</sub>, powdered and stored at -80°C until use.

### Leaf gas exchange, Chl $a$ fluorescence and metabolite analysis

Net CO<sub>2</sub> uptake ( $A$ ), stomatal conductance ( $g_s$ ) and transpiration rate ( $E$ ) were determined for the third fully expanded leaf (counting from the top) of at least three individuals using an infrared gas analyzer (Li 6400XT; Li-Cor, Lincoln, NE, USA). Measurements were performed between the second and the fifth hour after the onset of illumination, under controlled conditions of CO<sub>2</sub> concentration (380 ppm CO<sub>2</sub>), PFD  $\approx$  300  $\mu\text{mol m}^{-2} \text{s}^{-1}$  and chamber temperature of 25°C. Whenever relevant, continuous monitoring of net CO<sub>2</sub> uptake and transpiration rate over the 24 h cycle was also performed as described in Boxall *et al.* (2019). Chl $a$  fluorescence parameters were measured using a portable pulse amplitude modulation fluorometer (PAM-2500; Walz, Effeltrich, Germany) following the protocols and equations described by Alves *et al.* (2016). Values of minimal ( $F_o$ ) and maximal ( $F_m$ ) fluorescence were obtained from leaves dark-adapted for 30 min before receiving a saturating pulse of light (3000  $\mu\text{mol photons m}^{-2} \text{s}^{-1}$  for 1 s).

Titrate acidity analysis and organic acid and soluble carbohydrate profiling were performed as described in Freschi *et al.* (2010), with modifications described in Methods S1. Starch content was determined from dried pellets as described in Amaral *et al.* (2007). Whenever applicable, malate content was also quantified enzymatically as described in Boxall *et al.* (2019).

### Anatomical analyses

Leaves and stems were analyzed by light microscopy and scanning electron microscopy as described in Methods S1.

### RNA extraction and qPCR analysis

Total RNA was extracted using the ReliaPrep™ RNA Tissue Miniprep System (Promega), with modifications described in Methods S1. Complementary DNA (cDNA) synthesis and reverse-transcriptase quantitative polymerase chain reaction (qPCR) analysis were performed according to Cruz *et al.* (2018), with modifications described in Methods S1. All primer sequences used are listed in Table S1.

### RNA-seq *de novo* generation, assembly, annotation and analysis

Total RNA was extracted as described earlier from leaf and stem samples harvested in biological triplicates from well-watered and drought-stressed plants at D3 (08:00, 16:00 and 24:00 h, corresponding to 2 and 10 h after the onset of light, and 6 h into the 12 h dark period, respectively). Library preparation and

sequencing using the Illumina HiSeq4000 platform are detailed in Methods S1. RNA-seq assembly, annotation and all statistical analyses were performed as described in Methods S1. Fastq sequence files were deposited at NCBI under BioProject PRJNA576481.

### Identification of homologs and co-orthologs of CCM genes

Homologous and co-orthologous sequences related to genes encoding known CCM-related enzymes were identified as described in Moreno-Villena *et al.* (2017) with modifications described in Methods S1.

## Results

### Assessing CAM induction in *P. oleracea* leaves and stems during progressive drought treatment

Well-watered *P. oleracea* leaves showed atriplicoid-type anatomy, high daytime CO<sub>2</sub> uptake rates, and did not accumulate acids overnight (Fig. 1), confirming the use of C<sub>4</sub> whenever water was not limiting. By contrast, 34 d of water withholding promoted significant leaf nocturnal malic acid accumulation ( $\Delta\text{H}^+$ ) as detected via either enzymatic (Fig. 1b) or chromatographic (Fig. S1a) malate quantification and titratable acidity analysis (Fig. S1b), which was associated with no diel leaf gas exchange (Fig. 1c), thereby characterizing a CAM idling state (Winter, 2019). Crassulacean acid metabolism expression was upregulated rather than induced in *P. oleracea* stems in response to drought, probably relying on internal refixation of respiratory CO<sub>2</sub> as the stems lacked stomata (Fig. S2c,d). Kranz anatomy traits were absent in stems, in which  $\Delta\text{H}^+$  detected under well-watered conditions was significantly intensified upon drought (Fig. 1a,b), and chloroplasts are mainly distributed in cells of the inner cortex (Fig. S2g,h).

### Global transcriptional changes in response to drought

To gain an insight into the transcriptional changes associated with C<sub>4</sub> and CAM functioning in *P. oleracea*, RNA-seq was performed using leaf and stem RNA samples isolated from well-watered and drought-stressed plants harvested at 08:00, 16:00 and 24:00 h. A total of 1061 191 351 reads were obtained from all 36 libraries. Our *de novo* assembly for *P. oleracea* yielded 452 522 contigs, of which 84 494 were kept after open reading frame identification and redundancy elimination (Table S2). In all, 52 514 contigs were successfully annotated against the UniProt database and 80.35% of trimmed reads of all samples were mapped against our *de novo* assembly. Only the longest isoform for each annotated contig was kept (see Methods S1 for details), resulting in a total of 32 306 contigs.

Differentially expressed contigs in response to drought were identified at each sampling time point, revealing that *c.* 6% and 14% of the whole transcriptome were downregulated upon drought in leaves and stems, respectively (Fig. S3a; Table S3). Enrichment analysis for gene ontology (GO) terms revealed that photosynthesis

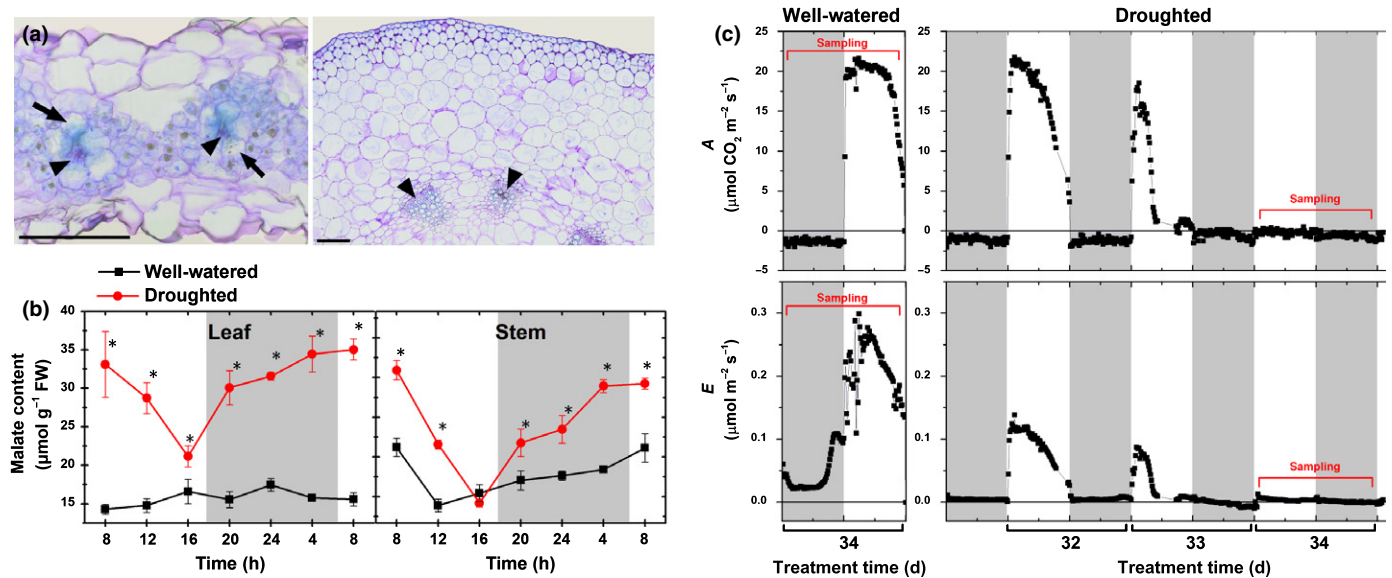


**Fig. 1** Drought promotes crassulacean acid metabolism (CAM) induction in  $C_4$  leaves and intensifies CAM expression in stems of *Portulaca oleracea*. (a) Leaf (left) and stem (right) cross-sections of well-watered plants. Black arrows and arrowheads indicate bundle sheath cells and vascular bundles, respectively. Bars, 250  $\mu\text{m}$ . (b) Diel fluctuation of malate content in leaf and stem from plants exposed to 34 d of well-watered or droughted treatments. Malate was determined via enzymatic assays. In (b), data are means ( $\pm$  SE) of at least three biological replicates and asterisks indicate significant difference ( $P < 0.05$ ). (c) Diel net  $\text{CO}_2$  assimilation (A) and transpiration (E) in leaves of plants exposed to well-watered or droughted treatments. In (c), data are normalized against the leaf area. In (b, c), the shaded areas indicate the dark period.

and sugar metabolism-related terms were particularly downregulated in drought-stressed leaves (Table S4), which agrees with the negative influence of drought on leaf  $\text{CO}_2$  assimilation (Fig. 1c). Photosynthesis- and carbohydrate metabolism-related GO terms were also enriched in well-watered leaves compared with well-watered stems (Table S4), reinforcing the fact that, although photosynthetically active, *P. oleracea* stems play a minor role in the overall shoot C fixation compared with the leaves.

The mean correlation coefficients obtained by comparing  $\log_2(\text{fold-change})$  ( $\log_2\text{FC}$ ) values from RNA-seq and  $\log_2$  ratio of mRNA relative abundance from qPCR analysis revealed adequate correspondence between RNA-seq and qPCR data in both leaf and stem samples (Fig. S4).

### Using transcriptomic data to identify CCM-related genes

Multiple approaches were employed to identify key candidate genes involved in *P. oleracea* CCM reactions. First, genes encoding major  $C_4$ /CAM-related genes were filtered according to annotation (Table S5), and the most representative contig for each gene was selected based on transcript abundance and  $\log_2\text{FC}$  (Figs 2, 4, S5, S6). Second, gene nomenclature was established according to Christin *et al.* (2014), based on phylogenetic trees inferred using data from  $C_3$ ,  $C_4$  and CAM plants. Groups of orthologs for selected CCM genes (Figs S7, S8) matched those previously identified for *Portulaca* (Christin *et al.*, 2014, 2015). Third, CCM genes differentially regulated by drought were further analyzed via qPCR for a detailed characterization of their diel cycles of transcript abundance (Figs 3, 5).

A typical  $C_4$ -like transcript abundance pattern was observed for CCM genes downregulated by drought (Fig. 2a), as they were

more abundant in leaves (Fig. 2b) and accumulated overnight, reaching a peak level phased to dawn (Fig. 3a), thereby preceding the start of  $C_4$  reactions. By contrast, fewer CCM genes were significantly upregulated following drought in both organs (Fig. 2a) and peaked in the dark (Fig. 3b), coinciding with the nocturnal acid accumulation promoted by drought in *P. oleracea* leaves and stems (Fig. 1b).

In both CCMs,  $\text{CO}_2$  can be converted to  $\text{HCO}_3^-$  passively or enzymatically by a beta-carbonic anhydrase ( $\beta\text{CA}$ ).  $\text{HCO}_3^-$  is combined with PEP by PPC to generate oxaloacetate (OAA) (Hatch, 1987). Although shared by both CCMs, these reactions occur at different times over the 24 h light : dark cycle in  $C_4$  and CAM, namely in the light and the dark, respectively. Among *P. oleracea*  $\beta\text{CA}$ - and PPC-encoding genes,  $\beta\text{CA-2E3}$  and  $\text{PPC-1E1a}'$  exhibited a  $C_4$ -like expression pattern, whereas  $\beta\text{CA-1E1}$  and  $\text{PPC-1E1c}$  were expressed in a CAM-like fashion (Fig. 2), reinforcing previous evidence that specific gene family members may have been recruited to fulfill the  $C_4$  and CAM carboxylation reactions according to the prevailing environmental conditions (Christin *et al.*, 2014).

*PPCK* is induced by high light in  $C_4$  leaves (Carter *et al.*, 1991). By contrast, *PPCK* expression is mainly controlled by the endogenous circadian clock in CAM species, leading to a dark-phased peak of *PPCK* activity, which promotes PPC phosphorylation and consequently increases the inhibitory constant ( $K_i$ ) of PPC for feedback inhibition by L-malate (Hartwell *et al.*, 1996; Hartwell *et al.*, 1999). In *P. oleracea*, RNA-seq data revealed a single *PPCK* ortholog (*PPCK-1E*), which showed transcript abundances that peaked 2 h into the 12 h light period (08:00 h) in  $C_4$ -performing leaves and peaked 16 h later (at 24:00 h) in CAM-performing leaves and stems (Figs 3c, S5).

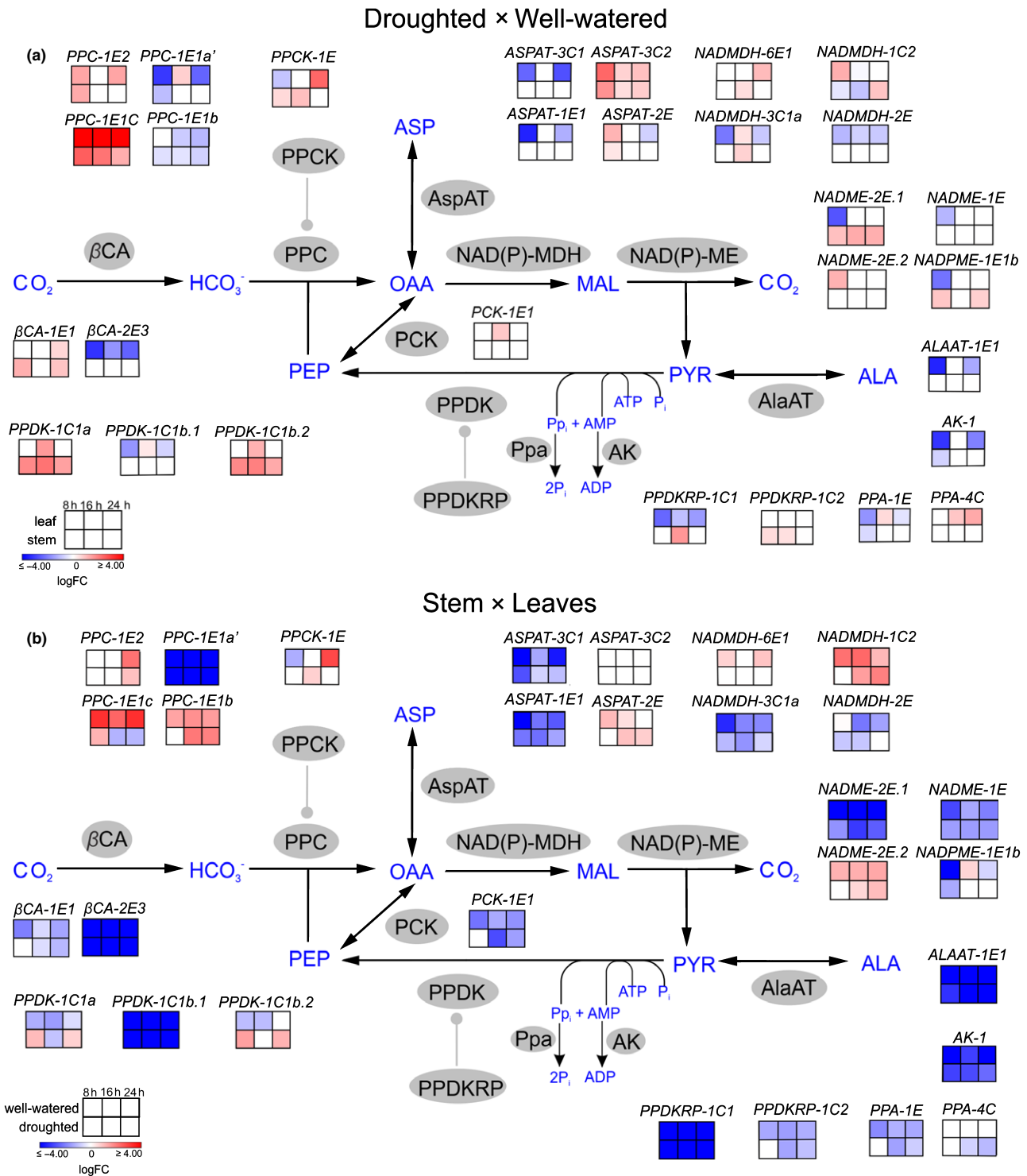


**Fig. 2** Drought-induced changes in transcriptional profile reveal key components of the C<sub>4</sub>/crassulacean acid metabolism (C<sub>4</sub>/CAM) machineries in *Portulaca oleracea*. Leaf and stem samples were harvested from plants maintained for 34 d under well-watered or droughted conditions. (a) Heatmaps indicate log<sub>2</sub>(fold-change) of droughted samples compared with well-watered samples. (b) Heatmaps indicate log<sub>2</sub>(fold-change) of stem samples compared with leaf samples. Black arrows indicate core reactions in both C<sub>4</sub> and CAM biosynthetic pathways whereas gray lines terminated by a closed circle indicate regulatory interactions. Intermediate reactions are omitted. Biosynthetic enzymes and metabolites are represented by gray ovals and blue letters, respectively. Trimmed Mean of M-values (TMM) and log<sub>2</sub>(fold-change) values for genes shown in the heatmaps are presented in Supporting Information Table S5 and Fig. S5, and their phylogenetic relationship is presented in Fig. S7. Statistically significant differences in comparison with well-watered (a) or leaf (b) samples are represented as colored squares (adjusted *P*-value < 0.05). Data are means (± SE) of at least three replicates. Metabolites: ALA, alanine; ASP, aspartate; OAA, oxaloacetate; MAL, malate; PEP, phosphoenolpyruvate; Ppa, inorganic pyrophosphatase; PYR, pyruvate. Enzymes: AK, adenylate kinase; ALAAT, ALA aminotransferase; ASPAT, ASP aminotransferase; βCA, beta-carbonic anhydrase; NAD(P)ME, NAD(P)-malic enzyme; NADMDH, NAD-malate dehydrogenase; PCK, PEP carboxykinase; PPC, PEP carboxylase; PPCK, PPC kinase; PPK-1E1, PPK regulatory protein.

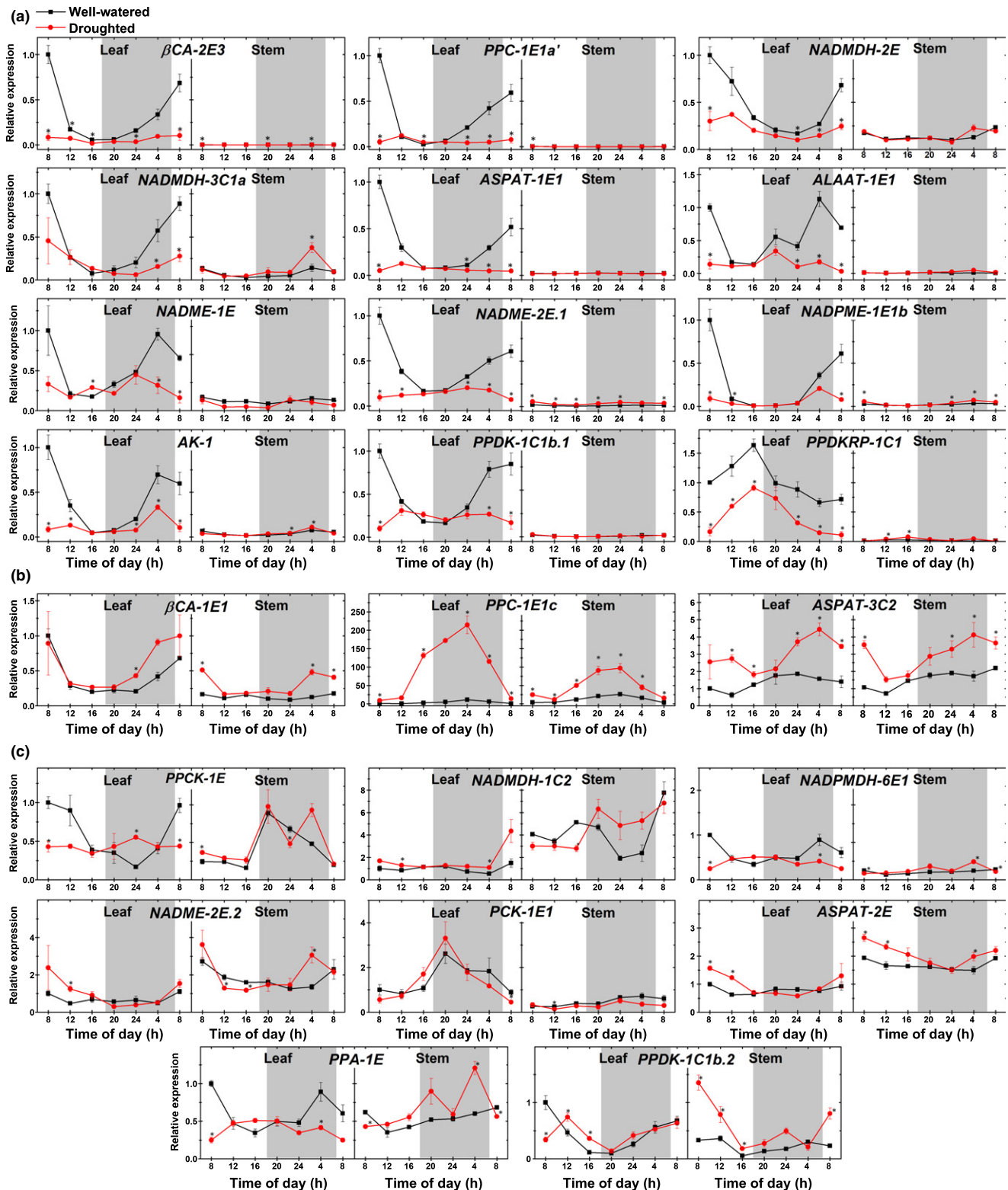


**Fig. 3** Drought induces changes in diel transcript abundance of key  $C_4$ /crassulacean acid metabolism ( $C_4$ /CAM) genes in *Portulaca oleracea*. (a) Reverse-transcriptase quantitative polymerase chain reaction (qPCR) data of genes exhibiting  $C_4$ -like expression patterns. (b) qPCR data of genes exhibiting CAM-like expression patterns. (c) qPCR data of other carbon-concentrating mechanism (CCM) genes. Mean relative expression in leaf and stem samples was normalized against the first time point (08:00 h) of well-watered leaf samples. The shaded areas indicate the dark period, and asterisks indicate significant difference ( $P < 0.05$ ). Data are means ( $\pm$  SE) of at least three replicates. AK, adenylate kinase protein; ALAAT, alanine aminotransferase; ASPAT, aspartate aminotransferase;  $\beta$ CA, beta-carbonic anhydrase; NAD(P)ME, NAD(P)-malic enzyme; NADMDH, NAD-malate dehydrogenase; PCK, phosphoenolpyruvate carboxykinase; Ppa, inorganic pyrophosphatase; PPC, phosphoenolpyruvate carboxylase; PPK, pyruvate orthophosphate dikinase; PPKRP, PPK regulatory protein.

C<sub>4</sub> species can use either NAD-malic enzyme (NAD-ME) or NADP-ME as primary decarboxylation enzymes with or without the additional involvement of PEP carboxykinase (PCK) (Furbank, 2011). *Portulaca oleracea* has been classified as a NAD-ME-type species (Lara *et al.*, 2004; Voznesenskaya *et al.*, 2010), implying that most CO<sub>2</sub> incorporated as OAA in this species is converted to aspartate (ASP) in MCs via aspartate aminotransferase (AspAT) activity. The ASP formed diffuses to BSCs via plasmodesmata and enters the mitochondria, where AspAT reverts ASP to OAA, and NAD-malate dehydrogenase (MDH) converts OAA to malate, which is decarboxylated by NAD-ME (Kanai & Edwards, 1999). To sustain these reactions, ASP and malate movements across mitochondria are facilitated by Uncoupling protein 2 (UCP2), Dicarboxylate transport 1 (DIT1) and Dicarboxylate carrier (DIC) proteins, respectively (Vozza *et al.*, 2014; Monné *et al.*, 2018; Palmieri *et al.*, 2008). Transcripts encoding enzymes and transporters characteristic of NAD-ME-type photosynthesis (*ASPAT-1E1*, *NADMDH-2E*, *NADMDH-3C1a*, *NADME-1E*, *NADME-2E.1*, *UCP-2* and *DIC-1.2*) were abundant in well-watered leaves and exhibited C<sub>4</sub>-like diel regulation, with peak levels phased to 08:00 h, 2 h into the 12 h light period (Figs 2–5). By contrast, *ASPAT-3C2* was upregulated significantly by drought in both leaves and stems, with a transcript peak phased to the second half of the dark period (Fig. 3b). However, ASP to OAA interconversion via AspAT is not part of the canonical CAM cycle, and *ASPAT-3C2* is phylogenetically closest to Arabidopsis *ASP3* (AT5G11520) (Fig. S7), which encodes a peroxisomal and chloroplastic protein implicated in photorespiration and senescence processes (Fukao *et al.*, 2002, Schultz & Coruzzi 1995; Wilkie & Warren 1998). Therefore, it seems unlikely that *ASPAT-3C2*-encoded protein is directly involved in *P. oleracea* CAM machinery.

Other genes, including *NADMDH-1C2*, *NADMDH-6E1* and *NADME-2E.2*, could be either shared by both CCMs or responsible for anaplerotic reactions as they did not show a clear pattern of modulation by drought (Figs 3c, S5). Transcripts of a NADP-ME-encoding gene (*NADPME-1E1b*) were abundant in both C<sub>4</sub>- and CAM-performing tissues (Fig. S5), but *NADPME-1E1b* is phylogenetically closest to Arabidopsis *NADP-ME4* (AT1G79750) (Fig. S7), which is implicated in fatty acid biosynthesis (Wheeler *et al.*, 2005). The only PCK-encoding gene identified (*PCK-1E1*) was a low-abundance transcript compared with other decarboxylases (Fig. S5), suggesting a limited, if any, contribution of PCK for decarboxylation reactions in this species.

In C<sub>4</sub> plants such as *P. oleracea*, after CO<sub>2</sub> is released by NAD-ME, the residual pyruvate (PYR) is transported to the cytosol by an unknown transporter, converted to alanine (ALA) by ALA aminotransferase (AlaAT) to flow back to MCs and be reverted to PYR again, finally entering the chloroplast (Kanai & Edwards, 1999). PYR is imported into the chloroplast in exchange of sodium by the bile acid:sodium symporter family protein (BASS), functioning in concert with the sodium:hydrogen antiporter (NHD) (Furumoto *et al.*, 2011). PEP supply is restored via PPK, releasing pyrophosphate and adenosine monophosphate (AMP), which are further metabolized via pyrophosphorylase and AMP kinase (AK) activities, respectively

(Matsuoka, 1995). PEP is then exported to the cytosol by PEP/phosphate translocator (PPT) (Thompson *et al.*, 1987). Genes encoding this suite of enzymes (*ALAAT-1E1*, *PPDK-1C1b.1*, *PPA-1E*, *AK-1*) and transporters (*BASS-1* and *PPT-1E2*) were abundant transcripts that displayed a C<sub>4</sub>-like temporal pattern in well-watered leaves (Figs 2–5). In response to drought, *BASS-1*, *PPT-1E2*, *ALAAT-1E1* and *AK-1* were downregulated in leaves, whereas *PPA-4C* was upregulated by drought in leaves (Fig. 2a) and *PPA-1E* and *PPDK-1C1b.2* were upregulated by drought in stems (Fig. 3c). As PPK activity is required in the daytime in both C<sub>4</sub> and CAM systems (Chastain *et al.*, 2002; Dever *et al.*, 2015), the *PPDKRP-1C1* transcript peak detected at the end of the light period (Fig. 3a) is consistent with the fact that PPK needs to be activated in the light and inactivated in the dark in both C<sub>4</sub> and CAM. Similar diel transcript abundance patterns have also been reported previously for *PPDKRP*-encoding genes in C<sub>4</sub> and CAM species (Chastain & Chollet, 2003; Dever *et al.*, 2015).

In CAM plants, malate accumulates as vacuolar malic acid as a result of nocturnal CO<sub>2</sub> fixation, and is subsequently released from the vacuole in the light period. The most likely candidates for nocturnal voltage-gated uptake of malate are the tonoplast-localized aluminum-activated malate transporters (ALMT) (Kovermann *et al.*, 2007; Borland *et al.*, 2009). Also, the tonoplast dicarboxylate transporter (TDT) may function in the transport of malate out of the vacuole for decarboxylation in the light period (Borland *et al.*, 2009). In *P. oleracea*, *ALMT-12E.1* and *ALMT-9E* were upregulated by drought in both leaf and stem tissues, whereas the opposite was observed for *ALMT-12E.2*, which was most abundant at the start of the light period in leaves under well-watered conditions (Figs 4, 5, S6). Among *ALMT* genes, *ALMT-9E* is closely related to Arabidopsis *ALMT9* (AT3G18440), a voltage-gated chloride channel in the tonoplast of guard cells (Zhang *et al.*, 2013), which has also been reported to act as a vacuolar malate channel in MCs (Kovermann *et al.*, 2007; De Angeli *et al.*, 2013). In addition to *ALMT* genes, *TDT-1E* was markedly upregulated by drought in stems, with a peak phased to 2 h before dawn (Figs 3, S6), which may suggest involvement in CAM.

Malate import into vacuoles in the dark period during CAM is mediated by a voltage-gated, inward-rectifying anion channel (Hafke *et al.*, 2003). The membrane potential difference across the tonoplast membrane that energizes this import is generated by the V-ATPase (also known as vacuolar-type proton ATPase (VHA)) and/ or the VPPase (pyrophosphate-energized membrane proton pump (AVP)) (Smith *et al.*, 1996). Drought promoted up- and downregulation of *VHAB2-1E1* and *AVP1-2E*, respectively (Figs 4, 5), and slightly increased transcript abundance for a range of other VHA subunit genes, including *VHAA3-3E*, *VHAF-1E* and *VHAG1-1E* (Fig. S6). Taken together, these results suggest a preference for VHA over AVP for the nocturnal accumulation of protons in the vacuole, which in turn energize nocturnal malate import via the putative tonoplast ALMT in CAM-performing *P. oleracea* tissues. It was noteworthy that *VHAB2-1E1* transcripts peaked in the middle of the night in drought-stressed leaves and stems of *P. oleracea* (Fig. 5b),

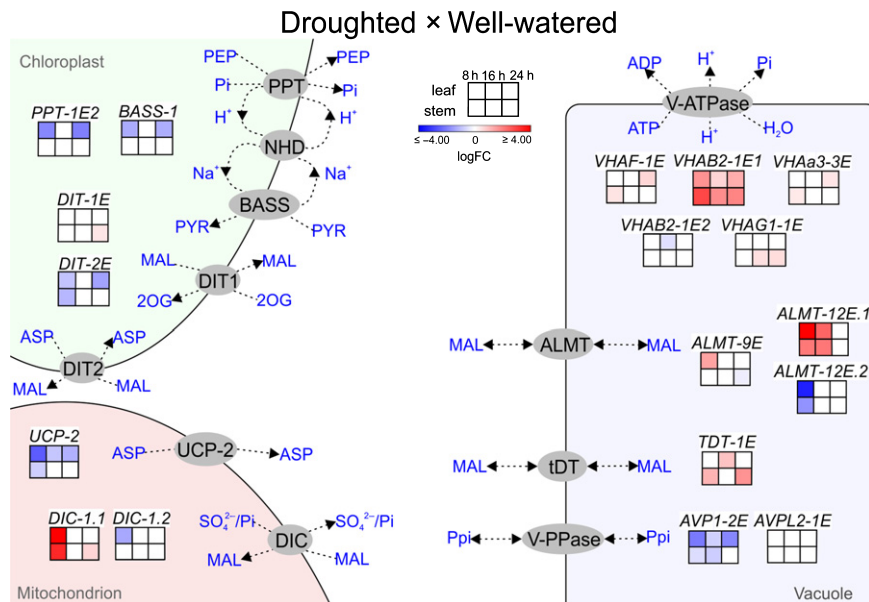


**Fig. 4** Drought modulates the transcriptional profile of genes encoding carbon-concentrating mechanism (CCM)-related transporters and pumps in *Portulaca oleracea*. Leaf and stem samples were harvested from plants maintained for 34 d under well-watered or droughted conditions. Schematic representation illustrating the putative intracellular localization of  $C_4$ /crassulacean acid metabolism ( $C_4$ /CAM)-related transporters and pumps, which are represented by gray ovals. Heatmaps indicate  $\log_2$ (fold-change) of droughted samples compared with well-watered samples. Trimmed Mean of  $M$ -values and  $\log_2$ (fold-change) values for genes shown in the heatmaps are presented in Supporting Information Fig. S6 and Tables S5 and S6, and their phylogenetic relationships are presented in Fig. S8. Statistically significant differences in comparison with well-watered samples are represented as colored squares (adjusted  $P$ -value  $< 0.05$ ). Data are means ( $\pm$  SE) of at least three replicates. Metabolites: 2OG, 2-oxoglutarate; ASP, aspartate; MAL, malate; OAA, oxaloacetate; PEP, phosphoenolpyruvate;  $P_i$ , inorganic phosphate. Transporters and pumps: ALMT, aluminum-activated malate transporter; BASS, sodium bile acid symporter family; DIC, dicarboxylate carrier; DIT, dicarboxylate transporter; PPT, PEP/phosphate translocator; PYR, pyruvate; tDT, tonoplast MAL/fumarate transporter; UCP-2, mitochondrial uncoupling protein 2; V-ATPase/VHA, V-type proton ATPase; V-PPase/AVP, pyrophosphate-energized membrane proton pump.

consistent with the proposed regulation of V-ATPase activity via the transcript abundance of the associated subunit genes (Chen *et al.*, 2012).

#### Temporal dynamics of photosynthetic transitions in response to water availability

Following the identification of signature  $C_4$  and CAM genes (Figs 2–5), we next performed comprehensive analysis of their temporal expression dynamics, aiming to determine whether  $C_4$  and CAM co-occur as drought conditions intensify, and whether CAM is reverted after rewatering events applied at distinct points of the drought treatment. Therefore, transcript abundance of CCM-marker genes, fluctuations in  $\Psi_s$ ,  $\Delta H^+$ , leaf gas exchange and Chl $a$  fluorescence were monitored in samples harvested after 0, 10, 22 and 34 d of drought treatment (D0, D1, D2 and D3, respectively) and during rewatering events initiated after 22 and 34 d of drought (R1 and R2, respectively).

Drought reduced plant growth, resulting in shorter shoots with fewer branches in comparison to well-watered plants (Fig. 6a). The prolonged maintenance of SVWC  $< 20\%$  field capacity (Fig. 6b) resulted in a significant decrease in both leaf and stem  $\Psi_s$  (Fig. 6c), which was associated with the reduction of  $A$ ,  $g_s$  and  $E$  values close to or below zero, the latter signifying the respiratory loss of  $CO_2$  from the leaf (Fig. 6d). In agreement,

leaf mRNA levels of genes encoding Rubisco small subunit (*RBCS*), Rubisco activase (*RCA*) and most photorespiration-related enzymes (Table S7), which were named according to phylogenetic analysis (Fig. S9), declined progressively in response to lengthening drought (Fig. S10).

Leaf transcript abundance of  $C_4$ -marker genes and daytime  $CO_2$  uptake was progressively reduced as drought intensified over time, whereas CAM-marker genes and  $\Delta H^+$  exhibited the opposite trend (Figs 6e–h, S11), indicating a gradual, rather than abrupt, intensification of CAM in leaves. Consequently, both physiological and gene transcript abundance data suggested that both CCMs may coexist in *P. oleracea* leaves under mild water deficit (D1). Furthermore, transcript abundances of  $C_4$ -related genes in leaves were still detected at *c.* 10–40% of their original abundance when maximum CAM expression had already been achieved (D2).

By contrast, drought-induced  $\Delta H^+$  and CAM-related transcript accumulation were rapidly and completely reversed upon rewatering (Fig. 6), regardless of the duration of the preceding drought treatment (R1 and R2). Within 1 and 2 d after rewatering, leaf  $\Psi_s$ , daytime  $CO_2$  uptake and  $C_4$ -related gene expression were fully re-established to levels similar to well-watered plants (Fig. 6). Therefore, CAM seems to be entirely replaced by  $C_4$  in leaves of *P. oleracea* soon after the water supply is re-established. By contrast, stems showed a progressive increase in both  $\Delta H^+$  and *PPC-1E1c* mRNA levels during plant growth under well-

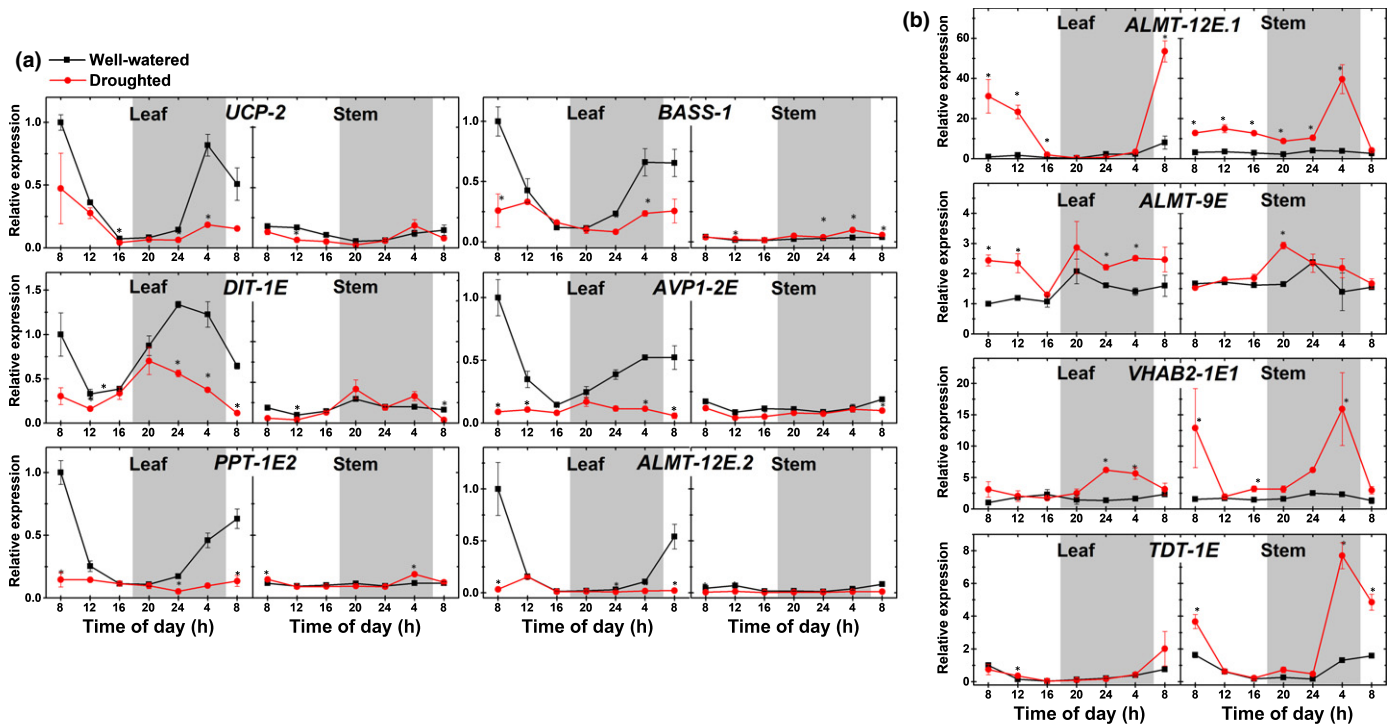


**Fig. 5** Diel transcript fluctuation of genes encoding carbon-concentrating mechanism (CCM)-related transporters and pumps is altered by drought in *Portulaca oleracea*. (a) Reverse-transcriptase quantitative polymerase chain reaction (qPCR) data of genes exhibiting C<sub>4</sub>-like expression patterns. (b) qPCR data of genes exhibiting crassulacean acid metabolism (CAM)-like expression patterns. Mean relative expression in leaf and stem samples was normalized against the first time point (08:00 h) of well-watered leaf samples. The shaded areas indicate the dark period and asterisks indicate significant difference ( $P < 0.05$ ). Data are means ( $\pm$  SE) of at least three replicates. ALMT, aluminum-activated malate transporter; BASS, sodium bile acid symporter family; DIT, dicarboxylate transporter; PPT, phospho $\pi$ pyruvatephosphate translocator; tDT, tonoplast malate/fumarate transporter; UCP-2, mitochondrial uncoupling protein 2; VHA, V-type proton ATPase; AVP, pyrophosphate-energized membrane proton pump.

watered conditions, which was intensified by drought (Fig. 6e,g), reinforcing that CAM expression in stem tissues is under both ontogenetic and environmental regulation.

The progressive decline in  $A$ ,  $g_s$ ,  $E$  and transcript abundances of *RBCS*, *RCA* and C<sub>4</sub>-signature genes in *P. oleracea* droughted leaves was not accompanied by significant changes in Chl $a$  fluorescence parameters such photochemical efficiency of the PSII ( $F_v/F_m$ ), PSII effective quantum yield ( $F_q/F_m$ ) and nonphotochemical quenching (Fig. S12). This suggests that linear electron transport within chloroplasts may have been maintained despite the drought-induced decline in atmospheric CO<sub>2</sub> uptake (Fig. 1c).

### Starch turnover intensified during CAM in *P. oleracea*

Transitory leaf starch metabolism is not as important for C<sub>4</sub> as it is for starch-storing CAM species, which require a sufficient pool size of starch at the start of each night in order to supply PEP to PPC throughout the dark period (Weise *et al.*, 2011). In line with these differential metabolic demands, a significant rewiring of carbohydrate-associated metabolism was observed during CAM induction and intensification in *P. oleracea* leaves and stems, respectively (Fig. 7; Table S8). Drought-promoted diel fluctuation in starch amounts was exclusively observed in stem tissues, achieving values up to two-fold higher in drought-stressed than in well-watered plants at the end of the light period, and declining to similar values in both watering conditions during

the first half of the dark period (Fig. 7a). Consequently, the drought-triggered increment in stem  $\Delta H^+$  coincided with an intensification in diel starch fluctuation. Crassulacean acid metabolism induction in leaves was instead associated with lower starch accumulation in leaves, which correlates with the progressive reduction in leaf photosynthetic C assimilation caused by drought-induced stomatal closure (Figs 1c, 6d).

Transcript abundances of contigs encoding both the small (*ADG1* and *ADG2*) and large (*APL3*) subunits of ADP-glucose pyrophosphorylase, the first committed step in starch biosynthesis, as well as Granule-bound starch synthase (*GBSSI*), responsible for amylose synthesis, peaked at 2 h into the light period, regardless of the tissue or watering condition (Fig. S13; Table S8). At this temporal peak, drought promoted transcript accumulation of *ADG1*, *APL3* and *GBSSI* in stems, but not in leaves (Figs 7b, S13). Transcript abundance of genes encoding enzymes involved in both the hydrolytic (amylolytic) and the phosphorolytic pathways of transitory starch degradation, including isoamylase 3 (*ISA3*), limit dextrinase or pullulase (*LDA*), disproportionating enzyme 1 (*DPE1*) and alpha-glucan water dikinase (*GWD*), were upregulated in both organs in response to drought (Fig. 7b; Table S8). Moreover, genes encoding enzymes associated with hydrolytic starch degradation (phosphoglucan phosphatase (*SEX4*), alpha-amylase (*AMY3*) and beta-amylase (*BAMI*)) as well as those required for the phosphorolytic pathway (starch phosphorylase1 (*PHS1*)) were also upregulated upon drought (Figs. 7b, S13).

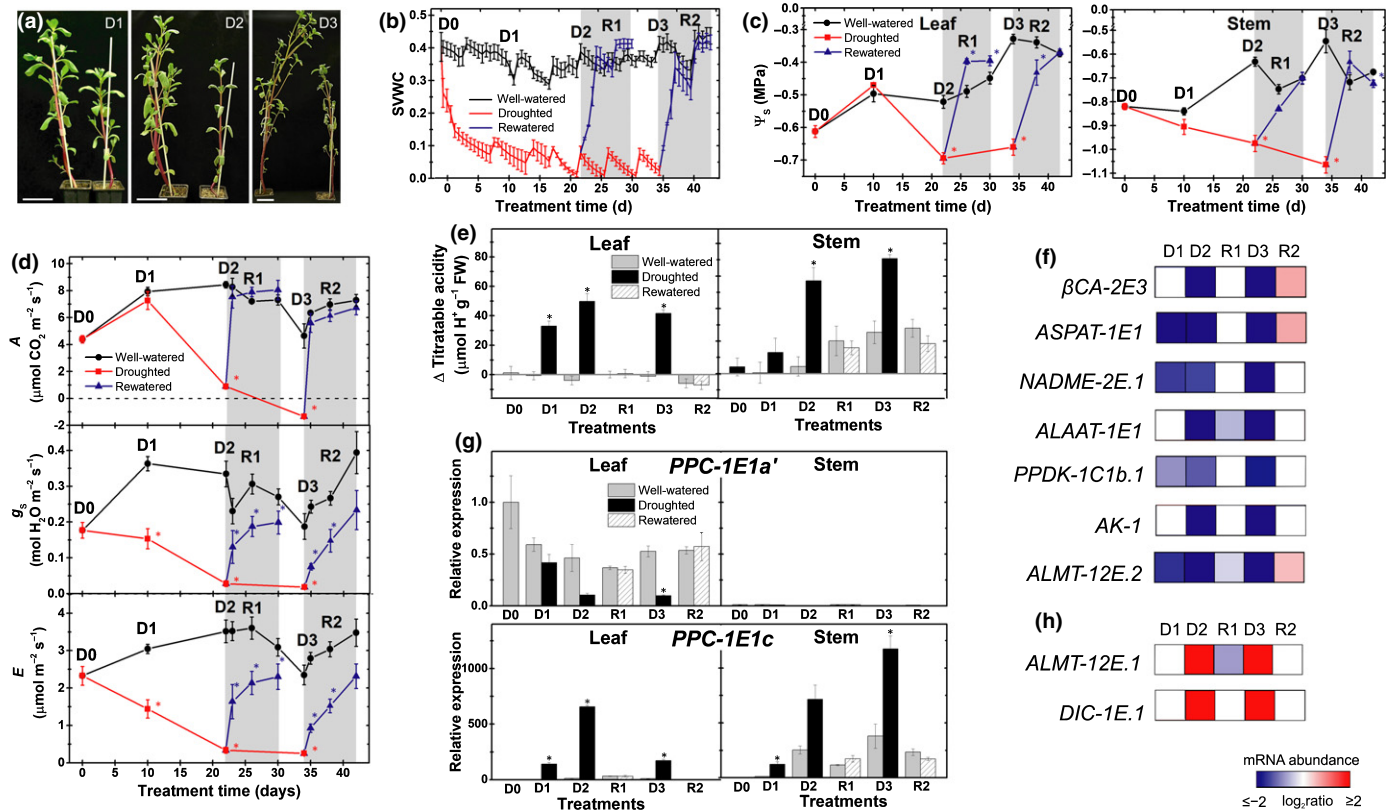


**Fig. 6** Changes in water availability promotes completely reversible photosynthetic transitions in *Portulaca oleracea*. Plants were sampled after 0, 10, 22 and 34 d of drought treatment (D0, D1, D2 and D3, respectively) and during rewatering events initiated after 22 and 34 d of drought (R1 and R2, respectively). (a) Overall morphological aspects of well-watered (left) and droughted (right) plants; bars, 7 cm; (b) soil volumetric water content (SVWC) during the treatments; (c) leaf and stem osmotic potential ( $\Psi_s$ ); (d) net  $\text{CO}_2$  uptake (A), stomatal conductance ( $g_s$ ) and transpiration (E) in leaves; (e) titrate acidity in leaf and stem tissues.  $\Delta \text{H}^+$  indicates dawn–dusk differences. In (e), SE of the dawn–dusk difference =  $\sqrt{(\text{SE}_{\text{dawn}})^2 + (\text{SE}_{\text{dusk}})^2}$ . (f) Heatmaps indicate  $\log_2$ (fold-change) of well-watered compared with drought/rewatered leaves for C<sub>4</sub>-signature genes (reverse-transcriptase quantitative polymerase chain reaction (qPCR) data are presented in Supporting Information Fig. S11). (g) Transcript abundance of phosphoenolpyruvate carboxylase (PPC)-encoding genes normalized against D0 leaf samples. (h) Heatmaps indicate  $\log_2$ (fold-change) of well-watered compared with drought/rewatered leaves for crassulacean acid metabolism (CAM)-signature genes (qPCR data are presented in Fig. S11). In (c–e, g), asterisks indicate significant difference ( $P < 0.05$ ). In (f, h), statistically significant differences are represented as colored squares (adjusted  $P < 0.05$ ). In (b–d), gray areas indicate rewatering events. Data are means ( $\pm$  SE) of at least three replicates. AK, adenylate kinase; ALAAT, alanine aminotransferase; ALMT, aluminum-activated malate transporter; ASPAT, aspartate aminotransferase;  $\beta\text{CA}$ , beta-carbonic anhydrase; DIC, dicarboxylate carrier; NAD-ME, NAD-malic enzyme; PPC, phosphoenolpyruvate carboxylase; PPDK, pyruvate orthophosphate dikinase.

Besides, chloroplast maltose exporter-encoding gene *MEX1* was predominantly downregulated upon drought, whereas *GPT2.2*, which encodes a G6P/phosphate translocator, was upregulated in both organs in response to drought (Figs 7b, S14).

Maltose can be converted to glucose via cytosolic disproportionating enzyme 2 (*DPE2*), starch phosphorylase 2 (*PHS2*) and phosphoglucomutase 2 (*PGM2*) (Brilhaus *et al.*, 2016). Transcripts encoding these three cytosolic enzymes remained unchanged or were downregulated in response to drought, whereas *PGM1*, which encodes a chloroplastic PGM, was upregulated by drought at dawn in both leaves and stems (Figs 7b, S13). The abundance of transcripts encoding cytosolic hexokinase 2 (*HXK2*), responsible for catalyzing the conversion of glucose to G6P (Brilhaus *et al.*, 2016), remained unchanged, whereas other *HXK* genes, such as *HXK1* (AT4G29130, nuclear localization) and *HXK3* (AT1G47840, chloroplastic), were only slightly modulated by drought. Glucose-6-phosphate isomerase

(PGI) can be either chloroplastic (*PGI1*) or cytosolic (*SIS.1* and *SIS.2*) and only the cytosolic forms were slightly upregulated in our transcriptome.

Despite the significant reduction in leaf and stem soluble sugar content following drought (Fig. 7a), genes encoding tonoplast sugar transporters, such as tonoplast monosaccharide transporters (*TMT*), early responsive to dehydration-like 6 (*ERDL6*) and *SWEET* (sugars will eventually be exported transporters), were predominantly upregulated upon drought, with the exception of *TMT1* and *SWEET16*. Variable transcript abundance patterns were also observed for genes encoding enzymes involved in glycolytic PEP production, with phosphofructokinase (*PFK6*), fructose-bisphosphate aldolase (*FBA6*) and triosephosphate isomerase (*TPI.1*) upregulated significantly in drought-stressed leaves 2 h before dusk (16:00 h) and in the middle of the dark period (24:00 h) (Figs 7b, S13; Table S8).

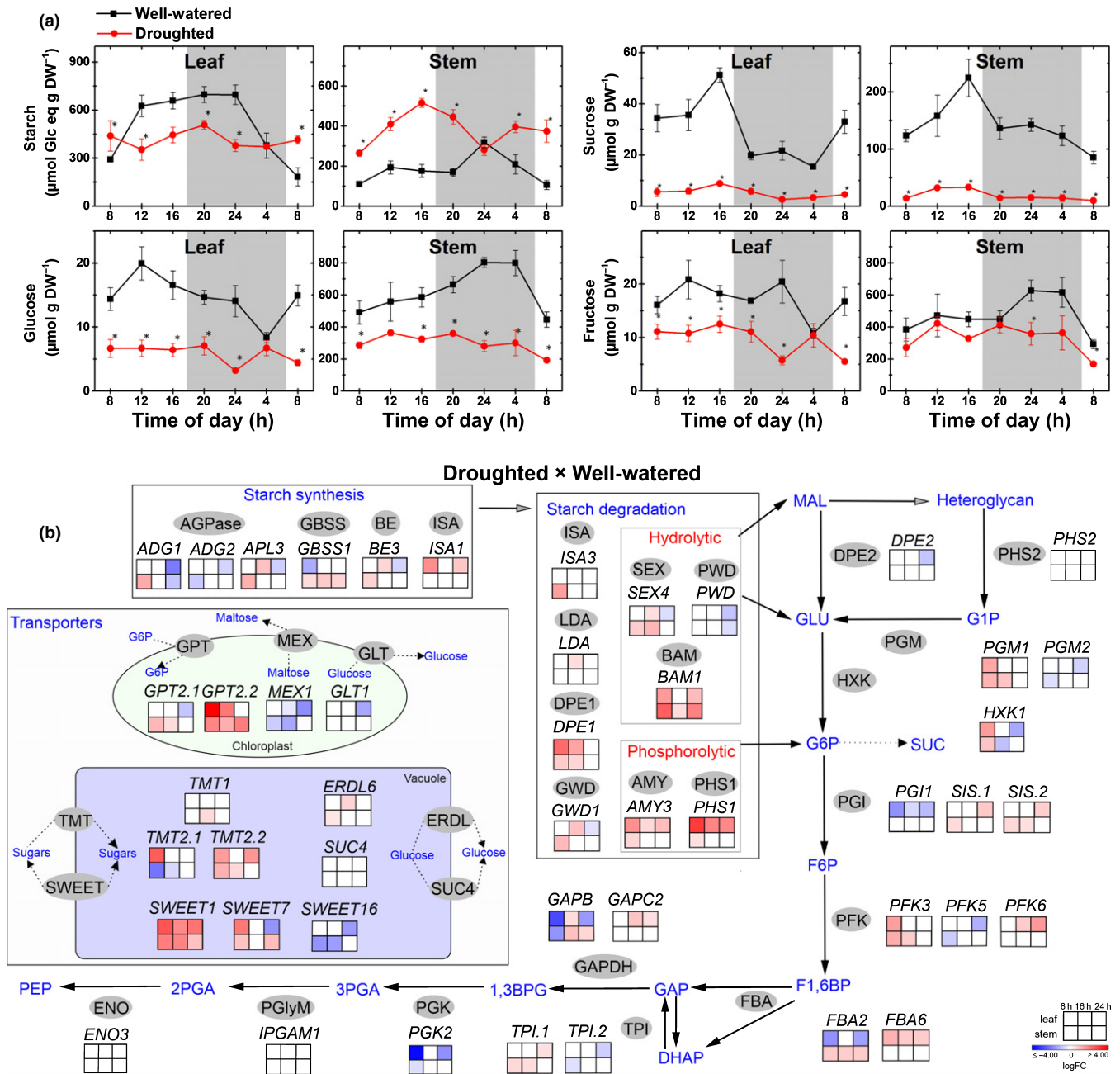


**Fig. 7** Coordinated changes in sugar metabolism accompany the drought-induced photosynthetic transitions of leaves and stems of *Portulaca oleracea*. Leaf and stem samples were harvested from plants maintained for 34 d under well-watered or drought conditions. (a) Diel fluctuations in starch, sucrose, glucose and fructose content. The shaded areas indicate the dark period and asterisks indicate significant difference ( $P < 0.05$ ). (b) Schematic representation of sugar metabolic reactions, with heatmaps indicating  $\log_2(\text{fold-change})$  of droughted samples compared with well-watered samples for leaves and stems. Biosynthetic enzymes and transporters are represented by gray ovals and intermediate reactions are omitted. Statistically significant differences are represented as colored squares (adjusted  $P < 0.05$ ). Gene names were assigned based on Arabidopsis closest homolog according to sequence similarity (see Supporting Information Methods S1). Trimmed Mean of M-values and  $\log_2(\text{fold-change})$  values for genes shown in heatmaps are presented in Table S8. Data are means ( $\pm$  SE) of at least three replicates. Metabolites: 1,3-BPG, 1,3-bisphosphoglycerate; 2-PGA, 2-phosphoglycerate; 3-PGA, 3-phosphoglycerate; DHAP, dihydroxyacetone phosphate; F1,6BP, fructose-1,6-bisphosphate; F6P, fructose-6-phosphate; G1P, glucose-1-phosphate; G6P, glucose-6-phosphate; GAP, glyceraldehyde 3-phosphate; GLU, glucose; MAL, maltose; PEP, phosphoenolpyruvate; SUC, sucrose. Enzymes: AGPase, G1P adenyltransferase; ADG, AGPase small subunit; APL, AGPase large subunit; AMY, amylase; BAM, beta-amylase; BE, starch branching enzyme; DPE, disproportionating enzyme; ENO, enolase; ERDL, vacuolar ERD6-like 6 glucose transporter; FBA, fructose-bisphosphate aldolase; GAPDH, GAP dehydrogenase; GBSS, granule-bound starch synthase; GLT, plastidic glucose transporter; GPT, G6P/phosphate translocator; GWD, alpha-glucan water dikinase; HXK, hexokinase; ISA, isoamylase; LDA, limit dextrinase; MEX, maltose exporter; PFK, 6-phosphofructokinase; PGI/SIS, G6P isomerase; PGK, phosphoglycerate kinase-2; PGlyM/IPGAM, phosphoglycerate mutase; PGM, phosphoglucanase; PHS, starch phosphorylase; PWD, phosphoglucan water dikinase; SEX, phosphoglucan phosphatase; SUC4, sucrose transport protein 4; SWEET, bidirectional sugar transporter; TMT, monosaccharide sensing protein; TPI, triosephosphate isomerase.

## Discussion

Species across the Caryophyllales comprise a hotspot for CCM evolution, including  $C_3$ ,  $C_3$ – $C_4$  intermediates, variations of  $C_4$  or CAM and even  $C_4$ –CAM facultative species, the latter occurring exclusively in *Portulaca* (Edwards & Ogburn, 2012). In *Portulaca*, CAM is believed to be ancestral to  $C_4$  considering its position relative to CAM-performing clades (e.g. cacti, *Ancampseros* and *Talinum*), and the evolution of biochemically and anatomically distinct  $C_4$  subtypes within the lineage (Voznesenskaya *et al.*, 2010; Christin *et al.*, 2014). Previous reports for *P. oleracea* (Koch & Kennedy, 1980; Mazen 1996, Lara *et al.*, 2003), as well as our current data, indicate that well-watered leaves perform  $C_4$ , whereas weak CAM is induced in both leaves and stems in response to drought.

Adding to the identification of two *P. oleracea* PPC genes recruited to function in the  $C_4$  and CAM cycles (Christin *et al.*, 2014), here we demonstrated contrasting diel cycling of transcript abundance for *PPC-1E1a'* compared with *PPC-1E1c*. Hence, the light/dark synchronization of the PPC-mediated primary carboxylation reactions in  $C_4$ - and CAM-performing leaves may, at least partially, rely on the opposite diel transcriptional regulation of these two PPC genes (Fig. 3). However, PPC is also post-translationally regulated, with PPCK-mediated PPC phosphorylation during the daytime ( $C_4$ ) or night-time (CAM), adjusting the enzyme's sensitivity to its allosteric inhibitor L-malate over the diel cycle (Nimmo *et al.*, 2001; Hibberd & Covshoff, 2010; Boxall *et al.*, 2017). Previously published results demonstrated that PPC kinetic properties, including its sensitivity to feedback inhibition by malate, activation by G6P, and affinity for PEP, were inverted relative to one another within the diel cycle as  $C_4$  was replaced by CAM in *P. oleracea* leaves (Mazen 1996, 2000). Our findings revealed that a single PPCK-encoding gene is shared by both CCMs, as *PPCK-1E1* mRNA accumulation coincided with  $C_4$  *PPC-1E1a'* accumulation in well-watered leaves and with CAM *PPC-1E1c* accumulation in droughted leaves.

Putative  $C_4$  signature genes were identified, including those implicated in carboxylation ( *$\beta$ CA-2E3*, *PPC-1E1a'*), acid formation (*ASPAT-1E1*, *NADMDH-2E*, *NADMDH-3C1a*, *ALAAT-1E1*), decarboxylation (*NADME-2E.1*) and PEP regeneration reactions (*AK-1*, *PPDK-1C1b.1*), as well as in the transport of PEP, ASP and PYR between subcellular compartments (*UCP-2*, *BASS-1*, *PPT-1E2*). Most reactions and processes associated with CAM functioning in *P. oleracea*, except for nocturnal carboxylation reactions (*PPC-1E1c*,  *$\beta$ CA-1E1*) and malate transport across the tonoplast (*ALMT-9E*, *VHAB2-1E1*, *TDT-1E*), were able to utilize genes shared by both CCMs. As drought-stressed *P. oleracea* display low-level diel acid fluctuation (weak CAM; Winter 2019), it probably demands reduced steady-state concentrations of dedicated enzymes to fulfill decarboxylation, PEP regeneration and other CAM cycle-related reactions.

The connectivity between  $C_4$  and CAM pathways in *P. oleracea* remains enigmatic and poorly investigated (Lara *et al.*, 2004; Christin *et al.*, 2014; Ferrari & Freschi, 2019). At one extreme,  $C_4$  and CAM pathways could be disconnected, never occurring at the same time and/or region of the mesophyll.

Alternatively, an interconnected  $C_4$ /CAM hybrid system might exist, in which several components and reactions would be shared between both CCMs. Within these extremes, any amount of  $C_4$ /CAM interconnection seems to be possible. Our findings support the temporal coexistence of both CCMs within *P. oleracea* leaves whenever water supply is restricted. We demonstrated that prolonged drought exposure promoted gradual, rather than abrupt, down- and upregulation of leaf  $C_4$  and CAM central components, respectively. Significant  $\Delta H^+$  and mRNA levels of CAM marker genes were observed as early as 10 d after water withholding, when diurnal  $CO_2$  uptake and  $C_4$  gene expression were only slightly reduced. Moreover, mRNA levels of  $C_4$  signature genes were still detectable when daytime gas exchange had ceased.

However, gathering reliable information about the tissue, cell type and subcellular distribution of  $C_4$  and CAM machineries within the *P. oleracea* leaf mesophyll remains critical for a full understanding of the interconnections between both CCMs. Therefore, the identification of CAM and  $C_4$  signature genes provided by this study provides a comprehensive set of candidates for future *in situ* hybridization and immunolocalization studies. Only one *in situ* immunolocalization study has been performed on drought-stressed *P. oleracea* leaves, which revealed that both Rubisco and NAD-ME were localized to the BSCs, whereas PPC was found in MCs and water storage cells (WSCs) (Lara *et al.*, 2004). Thus, instead of all CAM reactions taking place within a single cell (Winter & Smith 1996), an alternative two-cell  $C_4$ /CAM hybrid system has been proposed to operate in droughted *P. oleracea*. This hypothetical model proposes that malate accumulated overnight in vacuoles of MCs and WSCs would be transferred to BSCs during the light period for decarboxylation, providing  $CO_2$  to sustain Rubisco activity behind closed stomata (Lara *et al.*, 2004).

Although malate is typically transported from MCs to BSCs via plasmodesmata in  $C_4$  (Kanai & Edwards 1999), the  $C_4$ /CAM hybrid system would implicate additional metabolic fluxes, including the daily transport of malate stored at MCs, and possibly WSCs, to BSCs (Lara *et al.*, 2004). Interestingly, drought stress significantly impacted the transcript abundance of *P. oleracea* *ALMT-12E.1* and *ALMT-12E.2*, both closely related to Arabidopsis *ALMT12*, which encodes a plasma membrane malate transporter predominantly found in guard cells (Meyer *et al.*, 2010). As *P. oleracea* stems are devoid of stomata, the predominance of *ALMT-12E.2* transcripts in leaves suggests a functionally conserved role for this gene in controlling stomatal movements (Meyer *et al.*, 2010). By contrast, *ALMT-12E.1* transcripts were equally abundant in tissues containing or lacking stomata (leaves and stems, respectively), which may indicate functional divergence compared with Arabidopsis *ALMT12*. As *ALMT-12E.1* was highly induced by drought, it could suggest their involvement in the daytime transport of malate between WSCs, MCs and BSCs in *P. oleracea* leaves engaged in the  $C_4$ /CAM hybrid system.

Our data revealed completely reversible and environmentally controlled CAM in *P. oleracea* leaves, which agrees with previous findings for the species (D'Andrea *et al.*, 2014; Winter & Holtum, 2014). As no  $\Delta H^+$  or CAM-marker transcript

accumulation was observed after rewatering events applied following different lengths of the drought period, the ability of *P. oleracea* to revert from the C<sub>4</sub>/CAM hybrid system to C<sub>4</sub> was not influenced by the intensity or duration of CAM before rewatering. By contrast, both developmental and environmental cues were shown to regulate the occurrence and intensity of CAM in stems. As a consequence, multiple photosynthetic CO<sub>2</sub> fixation systems were detected in *P. oleracea*, including C<sub>3</sub> stems and C<sub>4</sub> leaves in young, well-watered plants, CAM stems and C<sub>4</sub> leaves in adult well-watered and rewatered plants, and CAM stems and C<sub>4</sub>/CAM hybrid leaves in adult, drought-stressed plants.

As stems represent up to 50% of *P. oleracea* total biomass (Zimmerman, 1976) and display  $\Delta H^+$  values as high as those found in droughted leaves (Fig. 6e), the presence of CAM in stem tissues could facilitate recycling the night-time respiratory CO<sub>2</sub> produced by its large chlorenchymatous cells. On the other hand, the adaptive value of facultative CAM in leaves is presumably similar for both C<sub>4</sub>-CAM and C<sub>3</sub>-CAM facultative plants. As other weak CAM facultative species, dark CO<sub>2</sub> fixation in drought-stressed, CAM-performing *P. oleracea* plants is negligible compared with daytime C<sub>4</sub>-mediated CO<sub>2</sub> assimilation under well-watered conditions (Winter & Holtum, 2014; Winter, 2019). Instead of contributing to C gain, weak and inducible CAM may promote plant fitness by offering other adaptive advantages (reviewed by Herrera, 2009). Our findings connect CAM induction to a photoprotective role in *P. oleracea* as the daytime CO<sub>2</sub> release from organic acids behind closed stomata may have supported linear electron transport within chloroplasts, maintaining the integrity of the photosynthetic apparatus under extreme drought as evidenced by Chl<sub>a</sub> fluorescence data (Fig. S12). The rapid recovery of photosynthetic rates once sufficient water supply becomes available may also be seen as an indicator of this photoprotective role of weak CAM (Adams & Osmond, 1988; Herrera, 2009).

Compared with CAM plants, PEP generation represents a much less significant sink for carbohydrates in C<sub>4</sub> plants as a result of the continuous daytime conversion of PYR to PEP by PPDK or its direct generation via PCK (Weise *et al.*, 2011; Borland *et al.*, 2016). In *Mesembryanthemum crystallinum*, where nocturnal malate accumulation contributes to plant C gain under stressful conditions (Bohnert & Cushman, 2000), incremental accumulation of starch during the C<sub>3</sub>-to-CAM switch seems essential for the supply of PEP (Haider *et al.*, 2012; Cushman *et al.*, 2008). By contrast, leaf starch concentrations either remained unchanged or were slightly reduced upon drought in weak CAM facultative species such as *Tallinum triangulare* (Brilhaus *et al.*, 2016) and *P. oleracea* (Fig. 7, D'Andrea *et al.*, 2014), accompanied by lower soluble sugar content, particularly sucrose and glucose, in both cases. In *P. oleracea* leaves, CAM induction was accompanied by the upregulation of most, but not all, starch metabolism genes (*ADG1*, *APL3*, *GBSS1*, *BE3*, *ISA3*, *GWD1*, *SEX4* and *BAMI*), as also observed for both *M. crystallinum* and *T. triangulare* (Cushman *et al.*, 2008; Brilhaus *et al.*, 2016). Therefore, an increased starch turnover, rather than a higher

accumulation of this carbohydrate, seems to be sufficient to sustain the dark CO<sub>2</sub> fixation and  $\Delta H^+$  observed in *P. oleracea*.

It has been hypothesized that a transition to phosphorolytic starch turnover favors the energetic balance for the nocturnal production of PEP from starch, requiring increased levels of GPT2, which transports G6P across the chloroplast envelope in exchange for inorganic phosphate (Neuhaus & Schulte, 1996; Cushman *et al.*, 2008; Borland *et al.*, 2009; Weise *et al.*, 2011). In *P. oleracea*, an overall increment in transcript abundance of *GPT2* as well as genes encoding enzymes either shared by both (*LDA*, *DPE1*, *GWD1*) or exclusively involved in the hydrolytic (*SEX4*, *BAMI*) and phosphorylytic (*PHS1*) starch degradation pathways was observed in response to drought. Therefore, both pathways seem to contribute to starch degradation in CAM-performing *P. oleracea* tissues. Additionally, the upregulation of *GPT2.2* may connect with the upregulation of cytosolic *SIS.1* and *SIS.2*, by transporting cytosolic G6P formed by SISs into the chloroplast to increase PEP regeneration via starch formation (Wai *et al.*, 2019).

Overall, our findings provide novel insights into the gene transcript abundance and metabolic adjustments required to accommodate both the C<sub>4</sub> and CAM cycles within a single leaf. In particular, our work builds on previous findings by identifying transcripts that are likely to play an exclusive role in drought-induced CAM reactions, as well as components that are shared by both the C<sub>4</sub> and CAM. By demonstrating that the C<sub>4</sub> and CAM machineries coexist within *P. oleracea* leaves under mild drought conditions, we open up a new window of opportunity for investigating the biochemical and regulatory mechanisms underpinning the co-occurrence of these two CCMs. Knowledge generated using C<sub>4</sub>/CAM facultative species such as *P. oleracea* may shed new light onto alternative biochemical arrangements for future bioengineering initiatives aiming to combine the high productivity of C<sub>4</sub> and the stress-resistance traits offered by CAM into target crop species.

## Acknowledgements

This work was supported in part by the São Paulo Research Foundation (FAPESP – grant no. 2016/04755-4 awarded to RCF), by a Newton Advanced Fellowship funded by the Royal Society, UK (grant no. NA140007 awarded to LF and JH) and by the US National Science Foundation (grant no. IOS-1754662 awarded to EJE). This study was financed in part by the Coordenação de Aperfeiçoamento de Pessoal de Nível Superior – Brasil (CAPES) – Finance Code 001. We also thank Nirja Kadu, Richard Eccles and Steve Paterson for the support given during the work at the Institute of Integrative Biology (University of Liverpool, UK), the members of the Centre for Genomic Research at the University of Liverpool that carried out the RNA-seq library production and Illumina sequencing, Emerson Alves da Silva (Instituto de Botânica de São Paulo) for support during osmotic potential measurements, and Luiz Lehmann Coutinho for granting access to the ESALQ Genomics Center Computer Cluster.

## Author contributions

LF and JH conceived the project and supervised the experiments; RCF and PPB conducted most of the experiments; MAR, LF, FRRA, DD, SFB, LVD, and JH conducted part of the experiments; SCSA conducted most bioinformatics analysis; VDG assisted the bioinformatic and statistical analysis; JJM-V and EJE performed the phylogenetic analyses; RCF, LF and JH wrote the article with contributions from other authors.

## ORCID

Frederico R. R. Alves  <https://orcid.org/0000-0002-2540-4699>  
 Sónia C.S. Andrade  <https://orcid.org/0000-0002-1302-5261>  
 Susanna F. Boxall  <https://orcid.org/0000-0002-8753-101X>  
 Diego Demarco  <https://orcid.org/0000-0002-8244-2608>  
 Louisa V. Dever  <https://orcid.org/0000-0001-7801-5622>  
 Renata C. Ferrari  <https://orcid.org/0000-0002-9497-8442>  
 Luciano Freschi  <https://orcid.org/0000-0002-0737-3438>  
 Vinícius D. Gastaldi  <https://orcid.org/0000-0002-6249-6035>  
 James Hartwell  <https://orcid.org/0000-0001-5000-223X>

## References

- Adams WW, Osmond CB. 1988. Internal CO<sub>2</sub> supply during photosynthesis of sun and shade grown CAM plants in relation to photoinhibition. *Plant Physiology* 86: 117–123.
- Alves FRR, Melo HC, Crispim-Filho AJ, Costa AC, Nascimento KJT, Carvalho RF. 2016. Physiological and biochemical responses of photomorphogenic tomato mutants (cv. Micro-Tom) under water withholding. *Acta Physiologiae Plantarum* 38: 155.
- Amaral LIV, Gaspar M, Costa PMF, Aider MPM, Buckeridge MS. 2007. Novo método enzimático rápido e sensível de extração e dosagem de amido em materiais vegetais. *Hoehnea* 34: 425–431.
- Black CC, Chen JQ, Doong RL, Angelov MN, Sung SJS. 1996. Alternative carbohydrate reserves used in the daily cycle of crassulacean acid metabolism. In: Winter K, Smith J, eds. *Crassulacean acid metabolism*. Heidelberg, Germany: Springer, 31–45.
- Bohnert HJ, Cushman JC. 2000. The ice plant cometh: lessons in abiotic stress tolerance. *Journal of Plant Growth Regulation* 19: 334–346.
- Borland AM, Griffiths H, Hartwell J, Smith JAC. 2009. Exploiting the potential of plants with crassulacean acid metabolism for bioenergy production on marginal lands. *Journal of Experimental Botany* 60: 2879–2896.
- Borland AM, Guo HB, Yang X, Cushman JC. 2016. Orchestration of carbohydrate processing for crassulacean acid metabolism. *Current Opinion in Plant Biology* 31: 118–124.
- Boxall SF, Dever LV, Kneřová J, Gould PD, Hartwell J. 2017. Phosphorylation of phosphoenolpyruvate carboxylase is essential for maximal and sustained dark CO<sub>2</sub> fixation and core circadian clock operation in the obligate crassulacean acid metabolism species *Kalanchoë fedtschenkoi*. *Plant Cell* 29: 2519–2536.
- Boxall SF, Kadu N, Dever LV, Kneřová J, Waller JL, Gould PJD, Hartwell J. 2019. Silencing PHOSPHOENOLPYRUVATE CARBOXYLASE1 in the obligate crassulacean acid metabolism species *Kalanchoë laxiflora* causes reversion to C<sub>3</sub>-like metabolism and amplifies rhythmicity in a subset of core circadian clock genes. *bioRxiv* 684050.
- Bräutigam A, Schlüter U, Eisenhut M, Gowik U. 2017. On the evolutionary origin of CAM photosynthesis. *Plant Physiology* 174: 473–477.
- Brillhaus D, Bräutigam A, Mettler-Altman T, Winter K, Weber APM. 2016. Reversible burst of transcriptional changes during induction of crassulacean acid metabolism in *Talinum triangulare*. *Plant Physiology* 170: 102–122.
- Carter PJ, Nimmo HG, Fewson CA, Wilkins MB. 1991. Circadian rhythms in the activity of a plant protein kinase. *EMBO Journal* 10: 2063–2068.
- Chastain CJ, Chollet R. 2003. Regulation of pyruvate, orthophosphate dikinase by ADP–Pi-dependent reversible phosphorylation in C<sub>3</sub> and C<sub>4</sub> plants. *Plant Physiology and Biochemistry* 41: 523–532.
- Chastain CJ, Fries JP, Vogel JA, Randklev CL, Vossen AP, Dittmer SK, Watkins EE, Fiedler LJ, Wacker SA, Meinhover KC *et al.* 2002. Pyruvate, orthophosphate dikinase in leaves and chloroplasts of C<sub>3</sub> Plants undergoes light–dark–induced reversible phosphorylation. *Plant Physiology* 128: 1368–1378.
- Chen Z, Hills A, Bätz U, Amtmann A, Lew VL, Blatt MR. 2012. Systems dynamic modeling of the stomatal guard cell predicts emergent behaviors in transport, signaling, and volume control. *Plant Physiology* 159: 1235–1251.
- Christin PA, Arakaki M, Osborne CP, Bräutigam A, Sage RF, Hibberd JM, Kelly S, Covshoff S, Wong GKS, Hancock L, *et al.* 2014. Shared origins of a key enzyme during the evolution of C<sub>4</sub> and CAM metabolism. *Journal of Experimental Botany* 65: 3609–3621.
- Christin PA, Arakaki M, Osborne CP, Edwards EJ. 2015. Genetic enablers underlying the clustered evolutionary origins of C<sub>4</sub> photosynthesis in angiosperms. *Molecular Biology and Evolution* 32: 846–858.
- Covshoff S, Hibberd JM. 2012. Integrating C<sub>4</sub> photosynthesis into C<sub>3</sub> crops to increase yield potential. *Current Opinion in Biotechnology* 23: 209–214.
- Cruz AB, Bianchetti RE, Alves FRR, Purgatto E, Peres LEP, Rossi M, Freschi L. 2018. Light, ethylene and auxin signaling interaction regulates carotenoid biosynthesis during tomato fruit ripening. *Frontiers in Plant Science* 9: 1–16.
- Cushman JC, Tillett RL, Wood JA, Branco JM, Schlauch KA. 2008. Large-scale mRNA expression profiling in the common ice plant, *Mesembryanthemum crystallinum*, performing C<sub>3</sub> photosynthesis and crassulacean acid metabolism (CAM). *Journal of Experimental Botany* 59: 1875–1894.
- D’Andrea RM, Andreo CS, Lara MV. 2014. Deciphering the mechanisms involved in *Portulaca oleracea* (C<sub>4</sub>) response to drought: metabolic changes including crassulacean acid-like metabolism induction and reversal upon re-watering. *Physiologia Plantarum* 152: 414–430.
- De Angeli A, Zhang J, Meyer S, Martinoia E. 2013. *AtALMT9* is a malate-activated vacuolar chloride channel required for stomatal opening in Arabidopsis. *Nature Communications* 4: 1–10.
- Dever LV, Boxall SF, Kneřová J, Hartwell J. 2015. Transgenic perturbation of the decarboxylation phase of crassulacean acid metabolism alters physiology and metabolism but has only a small effect on growth. *Plant Physiology* 167: 44–59.
- Edwards EL. 2019. Evolutionary trajectories, accessibility and other metaphors: the case of C<sub>4</sub> and CAM photosynthesis. *New Phytologist* 223: 1742–1755.
- Edwards EJ, Ogburn RM. 2012. Angiosperm responses to a low-CO<sub>2</sub> world: CAM and C<sub>4</sub> photosynthesis as parallel evolutionary trajectories. *International Journal of Plant Sciences* 173: 724–733.
- Ferrari RC, Freschi L. 2019. C<sub>4</sub>/CAM facultative photosynthesis as a means to improve plant sustainable productivity under abiotic-stressed conditions: regulatory mechanisms and biotechnological implications. In: Khan MIR, Reddy PS, Ferrante A, Khan NA, eds. *Plant signaling molecules*. Chennai, India: Woodhead Publishing, 517–532.
- Freschi L, Rodrigues MA, Tiné MAS, Mercier H. 2010. Correlation between citric acid and nitrate metabolisms during CAM cycle in the atmospheric bromeliad *Tillandsia pohlana*. *Journal of Plant Physiology* 167: 1577–1583.
- Fukao Y, Hayashi M, Nishimura M. 2002. Proteomic analysis of leaf peroxisomal proteins in greening cotyledons of *Arabidopsis thaliana*. *Plant Cell Physiology* 43: 689–696.
- Furbank RT. 2011. Evolution of the C<sub>4</sub> photosynthetic mechanism: are there really three C<sub>4</sub> acid decarboxylation types? *Journal of Experimental Botany* 62: 3103–3108.
- Furumoto T, Yamaguchi T, Ohshima-Ichii Y, Nakamura M, Tsuchida-Iwata Y, Shimamura M, Ohnishi J, Hata S, Gowik U, Westhoff P *et al.* 2011. A plastidial sodium-dependent pyruvate transporter. *Nature* 476: 472–476.
- Gonnella M, Charfeddine M, Conversa G, Santamaria P. 2010. Purslane: a review of its potential for health and agricultural aspects. *European Journal of Plant Science and Biotechnology* 4: 131–136.

- Griffiths H. 1989. Carbon dioxide concentrating mechanisms and the evolution of CAM in vascular epiphytes. In: Lüttge U, ed. *Vascular plants as epiphytes: evolution and ecophysiology*. Berlin, Germany: Springer, 42–86.
- Guralnick LJ, Jackson MD. 2001. The occurrence and phylogenetics of crassulacean acid metabolism in the Portulacaceae. *International Journal of Plant Sciences* 162: 257–262.
- Hafke JB, Hafke Y, Smith JAC, Lüttge UE, Thiel G. 2003. Vacuolar malate uptake is mediated by an anion-selective inward rectifier. *The Plant Journal* 35: 116–128.
- Haider MS, Barnes JD, Cushman JC, Borland AM. 2012. A CAM- and starch-deficient mutant of the facultative CAM species *Mesembryanthemum crystallinum* reconciles sink demands by repartitioning carbon during acclimation to salinity. *Journal of Experimental Botany* 63: 1985–1996.
- Hartwell J, Smith LH, Wilkins MB, Jenkins GI, Nimmo HG. 1996. Higher plant phosphoenolpyruvate carboxylase kinase is regulated at the level of translatable mRNA in response to light or a circadian rhythm. *The Plant Journal* 10: 1071–1078.
- Hartwell J, Gill A, Nimmo GA, Wilkins MB, Jenkins GI, Nimmo HG. 1999. Phosphoenolpyruvate carboxylase kinase is a novel protein kinase regulated at the level of expression. *The Plant Journal* 20: 333–342.
- Hartwell J. 2006. The circadian clock in CAM plants. In: Hall AJ, McWatters H, eds. *Annual plant reviews volume 21: endogenous plant rhythms*. Kundli, India: Blackwell Publishing, 211–236.
- Hartwell J, Dever LV, Boxall SF. 2016. Emerging model systems for functional genomics analysis of crassulacean acid metabolism. *Current Opinion in Plant Biology* 31: 100–108.
- Hatch MD. 1987. C<sub>4</sub> photosynthesis: a unique blend of modified biochemistry, anatomy and ultrastructure. *Biochimica et Biophysica Acta* 895: 81–106.
- Herrera A. 2009. Crassulacean acid metabolism and fitness under water deficit stress: if not for carbon gain, what is facultative CAM good for? *Annals of Botany* 103: 645–653.
- Hibberd JM, Covshoff S. 2010. The regulation of gene expression required for C<sub>4</sub> photosynthesis. *Annual Review of Plant Biology* 61: 181–207.
- Holtum JAM, Hancock LP, Edwards EJ, Winter K. 2017. Optional use of CAM photosynthesis in two C<sub>4</sub> species, *Portulaca cyclophylla* and *Portulaca digyna*. *Journal of Plant Physiology* 214: 91–96.
- Kajala K, Covshoff S, Karki S, Woodfield H, Tolley BJ, Dionora MJA, Mogul RT, Mabilangan AE, Danila FR, Hibberd JM *et al.* 2011. Strategies for engineering a two-celled C<sub>4</sub> photosynthetic pathway into rice. *Journal of Experimental Botany* 62: 3001–3010.
- Kanai R, Edwards GE. 1999. The biochemistry of photosynthesis. In: Sage R, Monson R, eds. *C<sub>4</sub> plant biology*. San Diego, CA, USA: Academic Press, 49–87.
- Keeley JE, Rundel PW. 2003. Evolution of CAM and C<sub>4</sub> carbon – concentrating mechanisms. *International Journal of Plant Sciences* 164: 54–77.
- Koch KE, Kennedy RA. 1980. Characteristics of crassulacean acid metabolism in the succulent C<sub>4</sub> dicot, *Portulaca oleracea* L. *Plant Physiology* 65: 193–197.
- Koch KE, Kennedy RA. 1982. Crassulacean acid metabolism in the succulent C<sub>4</sub> dicot, *Portulaca oleracea* L under natural environmental conditions. *Plant Physiology* 69: 757–761.
- Kovermann P, Meyer S, Hörtensteiner S, Picco C, Scholz-Starke J, Ravera S, Lee Y, Martinoia E. 2007. The Arabidopsis vacuolar malate channel is a member of the ALMT family. *The Plant Journal* 52: 1169–1180.
- Ku SB, Shieh YJ, Reger BJ, Black CC. 1981. Photosynthetic characteristics of *Portulaca grandiflora*, a succulent C<sub>4</sub> dicot. *Plant Physiology* 68: 1073–1080.
- Laetsch WM. 1968. Chloroplast specialization in dicotyledons possessing the C<sub>4</sub>-dicarboxylic acid pathway of photosynthetic CO<sub>2</sub> fixation. *American Journal of Botany* 55: 875–883.
- Lara M, Disante KB, Podestá FP, Andreo CS, Drincovich MF. 2003. Induction of a crassulacean acid like metabolism in the C<sub>4</sub> succulent plant, *Portulaca oleracea* L.: physiological and morphological changes are accompanied by specific modifications in phosphoenolpyruvate carboxylase. *Photosynthesis Research* 77: 241–254.
- Lara MV, Drincovich MF, Andreo CS. 2004. Induction of a crassulacean acid-like metabolism in the C<sub>4</sub> succulent plant, *Portulaca oleracea* L.: study of enzymes involved in carbon fixation and carbohydrate metabolism. *Plant and Cell Physiology* 45: 618–626.
- Matsuoka M. 1995. The gene for pyruvate, orthophosphate dikinase in C<sub>4</sub> plants: structure, regulation and evolution. *Plant and Cell Physiology* 36: 937–943.
- Mazen AMA. 1996. Changes in levels of phosphoenolpyruvate carboxylase with induction of crassulacean acid metabolism (CAM)-like behavior in the C<sub>4</sub> plant *Portulaca oleracea*. *Physiologia Plantarum* 98: 111–116.
- Mazen AMA. 2000. Changes in properties of phosphoenolpyruvate carboxylase with induction of crassulacean acid metabolism (CAM) in the C<sub>4</sub> plant *Portulaca oleracea*. *Photosynthetica* 38: 385–391.
- Meyer S, Mumm P, Imes D, Endler A, Weder B, Al-Rasheid KAS, Geiger D, Marten I, Martinoia E, Hedrich R. 2010. *AtALMT12* represents an R-type anion channel required for stomatal movement in Arabidopsis guard cells. *The Plant Journal* 63: 1054–1062.
- Miyanishi K, Cavers PB. 1980. The biology of canadian weeds. *Canadian Journal of Plant Science* 60: 953–963.
- Monné M, Daddabbo L, Gagneul D, Obata T, Hielscher B, Palmieri L, Miniero DV, Fernie AR, Weber APM, Palmieri F. 2018. Uncoupling proteins 1 and 2 (*UCP1* and *UCP2*) from *Arabidopsis thaliana* are mitochondrial transporters of aspartate, glutamate, and dicarboxylates. *Journal of Biological Chemistry* 293: 4213–4227.
- Moreno-Villena JJ, Dunning LT, Osborne CP, Christin PA. 2017. Highly expressed genes are preferentially co-opted for C<sub>4</sub> photosynthesis. *Molecular Biology and Evolution* 35: 94–106.
- Nelson EA, Sage TL, Sage RF. 2005. Functional leaf anatomy of plants with crassulacean acid metabolism. *Functional Plant Biology* 32: 409–419.
- Neuhaus HE, Schulte N. 1996. Starch degradation in chloroplasts isolated from C<sub>3</sub> or CAM (crassulacean acid metabolism)-induced *Mesembryanthemum crystallinum* L. *Biochemical Journal* 318: 945–953.
- Nimmo HG, Fontaine V, Hartwell J, Jenkins GI, Nimmo GA, Wilkins MB. 2001. PEP carboxylase kinase is a novel protein kinase controlled at the level of expression. *New Phytologist* 151: 91–97.
- Osmond CB. 1978. Crassulacean acid metabolism: a curiosity in context. *Annual Review of Plant Physiology* 29: 379–414.
- Palmieri L, Picault N, Arrigoni R, Besin E, Palmieri F, Hodges M. 2008. Molecular identification of three *Arabidopsis thaliana* mitochondrial dicarboxylate carrier isoforms: organ distribution, bacterial expression, reconstitution into liposomes and functional characterization. *Biochemical Journal* 410: 621–629.
- Sage RF. 2002. Are crassulacean acid metabolism and C<sub>4</sub> photosynthesis incompatible? *Functional Plant Biology* 29: 775–785.
- Sage RF. 2017. A portrait of the C<sub>4</sub> photosynthetic family on the 50<sup>th</sup> anniversary of its discovery: species number, evolutionary lineages, and hall of fame. *Journal of Experimental Botany* 68: e11–e28.
- Smith JAC, Ingram J, Tsiantis MS, Barkla BI, Bartholomew DM, Bettey M. 1996. Transport across the vacuolar membrane in CAM plants. In: Winter K, Smith J, eds. *Crassulacean acid metabolism*. Heidelberg, Germany: Springer-Verlag, 53–71.
- Schluter U, Denton AK, Bräutigam A. 2016. Understanding metabolite transport and metabolism in C<sub>4</sub> plants through RNA-seq. *Current Opinion in Plant Biology* 31: 83–90.
- Schultz CJ, Coruzzi GM. 1995. The aspartate aminotransferase gene family of Arabidopsis encodes isoenzymes localized to three distinct subcellular compartments. *The Plant Journal* 7: 61–75.
- Silvera K, Neubig KM, Whitten WM, Williams NH, Winter K, Cushman JC. 2010. Evolution along the crassulacean acid metabolism continuum. *Functional Plant Biology* 37: 995–1010.
- Taylor SH, Ripley BS, Martin T, De-WetLA, WoodwardFI, OsborneCP. 2014. Physiological advantages of C<sub>4</sub> grasses in the field: a comparative experiment demonstrating the importance of drought. *Global Change Biology* 20: 1992–2003.
- Thompson AG, Brailsford MA, Beechey RB. 1987. Identification of the phosphate translocator from maize mesophyll chloroplasts. *Biochemical and Biophysical Research Communications* 143: 164–169.
- Voznesenskaya EV, Franceschi VR, Kiirats O, Freitag H, Edwards GE. 2001. Kranz anatomy is not essential for terrestrial C<sub>4</sub> plant photosynthesis. *Nature* 414: 543–546.

- Voznesenskaya EV, Franceschi VR, Kiirats O, Artyusheva EG, Freitag H, Edwards GE. 2002. Proof of  $C_4$  photosynthesis without Kranz anatomy in *Bienertia cycloptera* (Chenopodiaceae). *The Plant Journal* 31: 649–662.
- Voznesenskaya EV, Koteyeva NK, Edwards GE, Ocampo G. 2010. Revealing diversity in structural and biochemical forms of  $C_4$  photosynthesis and a  $C_3$ – $C_4$  intermediate in genus *Portulaca* L. (Portulacaceae). *Journal of Experimental Botany* 61: 3647–3662.
- Zozza A, Parisi G, De Leonardi F, Lasorsa FM, Castegna A, Amorese D, Marmo R, Calcagnile VM, Palmieri L, Ricquier D *et al.* 2014. UCP2 transports  $C_4$  metabolites out of mitochondria, regulating glucose and glutamine oxidation. *Proceedings of the National Academy of Sciences, USA* 111: 960–965.
- Wai CM, Weise SE, Ozersky P, Mockler TC, Michael TP, VanBuren R. 2019. Time of day and network reprogramming during drought induced CAM photosynthesis in *Sedum album*. *PLoS Genetics* 15: e1008209.
- Weise SE, Van Wijk KJ, Sharkey TD. 2011. The role of transitory starch in  $C_3$ , CAM, and  $C_4$  metabolism and opportunities for engineering leaf starch accumulation. *Journal of Experimental Botany* 62: 3109–3118.
- Wilkie SE, Warren MJ. 1998. Recombinant expression, purification, and characterization of three isoenzymes of aspartate aminotransferase from *Arabidopsis thaliana*. *Protein Expression and Purification* 12: 381–389.
- Winter K. 2019. Ecophysiology of constitutive and facultative CAM photosynthesis. *Journal of Experimental Botany*. doi: 10.1093/jxb/erz002.
- Winter K, Smith J. 1996. Crassulacean acid metabolism: current status and perspectives. In: Winter K, Smith J, eds. *Crassulacean acid metabolism*. Heidelberg, Germany: Springer-Verlag, 1–13.
- Winter K, Holtum JAM. 2014. Facultative crassulacean acid metabolism (CAM) plants: powerful tools for unravelling the functional elements of CAM photosynthesis. *Journal of Experimental Botany* 65: 3425–3441.
- Winter K, Holtum JAM. 2017. Facultative crassulacean acid metabolism (CAM) in four small  $C_3$  and  $C_4$  leaf-succulents. *Australian Journal of Botany* 65: 3425–3441.
- Winter K, Sage RF, Edwards EJ, Virgo A, Holtum JAM. 2019. Facultative crassulacean acid metabolism in a  $C_3$ – $C_4$  intermediate. *Journal of Experimental Botany* 70: 6571–6579.
- Wheeler MCG, Tronconi MA, Drincovich MF, Andreo CS, Flügge U, Maurino VG. 2005. A comprehensive analysis of the NADP-malic enzyme gene family of *Arabidopsis*. *Plant Physiology* 139: 39–51.
- Yang X, Cushman JC, Borland AM, Edwards EJ, Wullschlegel SD, Tuskan GA, Owen NA, Griffiths H, Smith JAC, De Paoli HC *et al.* 2015. A roadmap for research on crassulacean acid metabolism (CAM) to enhance sustainable food and bioenergy production in a hotter, drier world. *New Phytologist* 207: 491–504.
- Zhang J, Baetz U, Krugel U, Martinoia E, De Angeli A. 2013. Identification of a probable pore-forming domain in the multimeric vacuolar anion channel *AtALMT9*. *Plant Physiology* 163: 830–843.
- Zimmerman CA. 1976. Growth characteristics of weediness in *Portulaca Oleracea* L. *Ecology* 57: 964–974.

## Supporting Information

Additional Supporting Information may be found online in the Supporting Information section at the end of the article.

**Fig. S1** Diel leaf acid fluctuation in well-watered and droughted plants.

**Fig. S2** Surface view and fluorescence microscopy of *P. oleracea* leaves and stems.

**Fig. S3** Differentially expressed genes across all pairwise comparisons.

**Fig. S4** Validation of RNA-seq data via qPCR.

**Fig. S5** Mean TMM values for contigs of CCM core reactions.

**Fig. S6** Mean TMM values for contigs of CCM-related transporter reactions.

**Fig. S7** Phylogenetic trees for genes encoding core CCM enzymes.

**Fig. S8** Phylogenetic trees for genes encoding CCM-related transporters and pumps.

**Fig. S9** Phylogenetic trees for genes encoding core photorespiration-related enzymes.

**Fig. S10** Relative abundance of genes encoding photorespiration-related enzymes.

**Fig. S11** Transcript abundance of  $C_4$  and CAM marker genes upon drought and rewatering.

**Fig. S12** *Chla* fluorescence in response to drought and rewatering.

**Fig. S13** Mean TMM values for contigs of carbohydrate metabolism genes.

**Fig. S14** Mean TMM values for contigs of genes encoding carbohydrate-related transporters.

**Methods S1** Extended description of materials and methods.

**Table S1** Primer sequences used for qPCR.

**Table S2** Overall sequencing statistics.

**Table S3** Annotation and abundance of all reads mapped to the *P. oleracea* transcriptome.

**Table S4** Gene ontology (GO) enrichment analysis.

**Table S5** Contigs annotated as part of key  $C_4$ /CAM modules.

**Table S6**  $C_4$ /CAM-related differentially expressed contigs in response to drought.

**Table S7** Photorespiration-related differentially expressed contigs in response to drought.

**Table S8** Carbohydrate-related differentially expressed contigs in response to drought.

Please note: Wiley Blackwell are not responsible for the content or functionality of any Supporting Information supplied by the authors. Any queries (other than missing material) should be directed to the *New Phytologist* Central Office.